



Cite this: *RSC Adv.*, 2022, **12**, 17715

Received 25th February 2022  
 Accepted 2nd June 2022

DOI: 10.1039/d2ra01273a  
[rsc.li/rsc-advances](http://rsc.li/rsc-advances)

## Echem methods and electrode types of the current *in vivo* electrochemical sensing

Qiuye Song,<sup>†,a</sup> Qianmin Li,<sup>†,b</sup> Jiadong Yan<sup>\*a</sup> and Yonggui Song<sup>ID, \*bc</sup>

For a long time, people have been eager to realize continuous real-time online monitoring of biological compounds. Fortunately, *in vivo* electrochemical biosensor technology has greatly promoted the development of biological compound detection. This article summarizes the existing *in vivo* electrochemical detection technologies into two categories: microdialysis (MD) and microelectrode (ME). Then we summarized and discussed the electrode surface time, pollution resistance, linearity and the number of instances of simultaneous detection and analysis, the composition and characteristics of the sensor, and finally, we also predicted and prospected the development of electrochemical technology and sensors *in vivo*.

### 1. Introduction

The *in vivo* continuous monitoring of chemical and biological species are urgently needed and have a profound impact in the field of life science, including medical diagnostics, pharmacological researches and physiology research. But the classical analytical methods are mostly limited to chromatographic methods which require expensive and cumbersome equipment such as (ultra) high-performance liquid chromatography (HPLC),<sup>1</sup> and (ultra) high-performance liquid chromatography-mass spectrometry (LC-MS),<sup>2-7</sup> etc. All of the above methods are very selective and reliable in terms of quantitative determination, but they always require extensive sample pretreatments such as extracting the animal body fluids or making tissue homogenates after the animal was executed, and then, through a series of complicated purification processes using one by one injection testing systems to detect and analyze biological samples. More details of the operation could be found in our previous work.<sup>1-4</sup> Therefore, it is of high cost, time-consuming and not easy to carry out continuous monitoring *in vivo*, moreover, the composition of the samples might change a lot with time elapsing in the handling process, and could not be a real-time reflection of the dynamic process of life information

*in vivo*. These shortcomings make the application of these methods severely limited.

*In vivo* electrochemistry not only brings relevant information about transmitter release, pathological markers and behavior, but also has developed many new methods to detect biological related molecules and manufacture high selective electrodes. Compared with the above large analytical instruments, electrochemical instruments have simpler and more economical advantages. For example, the traditional detection methods of MiRNA are northern hybridization, RT-PCR, etc. The northern hybridization operation is very cumbersome and the detection sensitivity is low. Although the detection limit of RT-PCR is low, the cost is high. The use of electrochemical sensors not only has higher sensitivity but also simple operation and lower detection cost (for example, tungsten oxide (WO<sub>3</sub>) is the main material of the sensor, which has the advantages of low cost, non-toxicity, abundant sources, simple preparation process, etc.).<sup>124</sup> Now *in vivo* electrochemistry has become the main medium of neuroscience.<sup>8</sup> Particularly, with the development of biosensors, through the modification of the new electrically conductive materials to immobilize the enzymes,<sup>9,10</sup> antibodies<sup>11</sup> and other biological materials<sup>12</sup> on the surface of the electrode, the sensitivity and selectivity of the electroanalytical method can be both improved, and it can not only detect the low-concentration and trace chemicals *in vivo*, but also resist the potential interferences from the many compounds presented in living body. More importantly, it does not need the complicated sample pretreatment.<sup>13</sup> Therefore, electrochemical measurement can help us solve the problems that cannot be solved by individual organisms: mixed sampling and whole tissue homogenization. At present, it has gradually become the most ideal real-time online detection technology.

This paper reviews the progress of new electrochemical sensing equipment and methods for biological samples in the

<sup>a</sup>The Affiliated Zhangjiagang Hospital of Soochow University, Zhangjiagang 215600, Jiangsu, People's Republic of China. E-mail: 34882311@qq.com; Fax: +86 791 87802135; Tel: +86 791 87802135

<sup>b</sup>Key Laboratory of Depression Animal Model Based on TCM Syndrome, Jiangxi Administration of Traditional Chinese Medicine, Key Laboratory of TCM for Prevention and Treatment of Brain Diseases with Cognitive Dysfunction, Jiangxi Province, Jiangxi University of Chinese Medicine, 1688 Meiling Road, Nanchang 330006, China

<sup>c</sup>Key Laboratory of Pharmacodynamics and Safety Evaluation, Health Commission of Jiangxi Province, Nanchang Medical College, 1688 Meiling Road, Nanchang 330006, China

<sup>†</sup> These authors contributed equally to this work.



past two decades, and reviews the development of electrochemical *in vivo* detection and analysis technology using biosensors and biological related molecules of electrochemical sensors and neurochemistry. The microdialysis technology, microfluidic chip, microelectrode and microelectrode array electrode manufacturing and modification are introduced. Some new electrochemical methods, methods to resist electrode biofouling<sup>15</sup> and improve sensitivity, and methods to measure the aluminum content in the microenvironment of the plant were introduced.<sup>14</sup> The current approach of electrochemical *in vivo* measurement are comprehensively reviewed here.

## 2. Microdialysis (MD)-electrochemical *in vivo* detection system

Microdialysis (MD) is a mature extraction technology that can monitor the dynamic changes of chemicals in the body. This technology originated in 1996. At that time Bito *et al.* Based on the principle of analyte diffusion on a porous membrane, they inserted sterile dialysis sacs into the dog's cortex so that the analytes were collected in a saline stream through the sterile dialysis sac, where they could then be detected.<sup>16,17</sup> Most polluting molecules, such as proteins, can be excluded from the lysate by this method under electrochemical conditions (Fig. 1), so this method can effectively avoid sensor pollution. At present, rapid microdialysis sampling has been widely used in cortical diffusion inhibition in cerebral cortex research.<sup>18</sup> In this case, by injecting potassium chloride solution, the dialysate is transported to the area where lactate and glucose are detected at the same time. Based on this principle, the depolarization of diffusion wave can be induced in animal model (here, cat), so that the levels of glucose and lactate can be detected. The experimental results showed that the brain tissue was likely to be seriously damaged because the glucose level decreased by 28% 10 minutes after cortical diffusion depolarization was induced, but the galactose level increased by 58%, and the glucose consumption in the brain tissue lasted for at least 30 minutes. Patients in the intensive care unit after acute brain injury also use the same method to detect glucose.<sup>19</sup> It is found that spontaneous brain injury is caused by depolarization, and the methods of increasing lactic acid and inhibiting hypoglycemia can effectively reduce brain injury. The device can detect cortical diffusion depolarization by combining with subdural EEG.

MD has the advantages of "*in vivo*, real-time, minimally invasive, trace detection, accurate and efficient", and can even make a at least 2 hours continues measurement.<sup>20-22</sup> At the same time, early microdialysis technology is often used for *in vivo* metabolic analysis of neurotransmitters such as dopamine and serotonin after administration.<sup>131,132</sup> During the conventional online measurements through the sampling technique of microdialysis, analytes in dialysate are always regularly measured by classical chromatographic methods such as (ultra) high performance liquid chromatography HPLC, and (ultra)

high performance liquid chromatography-mass spectrometry (LC-MS).<sup>2,23-25</sup> These approaches are inadequate for some applications, especially for some life science studies which require continuous monitoring, high temporal resolution and rapid experimental data collection. Some analytical chemistry scientists like Lanqun Mao<sup>26-28</sup> and Guoyue Shi<sup>29-32</sup> *et al.* have established a stable microdialysis online electrochemical testing platform for monitoring the dynamic changes of biologically relevant molecules in rat brain (*e.g.* hippocampal ascorbate<sup>30</sup> and striatum glucose,<sup>22,26,28,29</sup> dopamine,<sup>32</sup> glutamate,<sup>30,31</sup> *etc.*). Due to the continuous detection and simple sample pre-treatment characteristics of the electrochemical sensors, the MD-electrochemical sensors not only can extract the biological samples from a living body for direct analysis without any other pretreatments, but also monitor the biological events continuously at least 2 h.<sup>20-22</sup>

### 2.1 MD-thin-layer electrochemical flow-through cell (TEFC) *in vivo* detection system

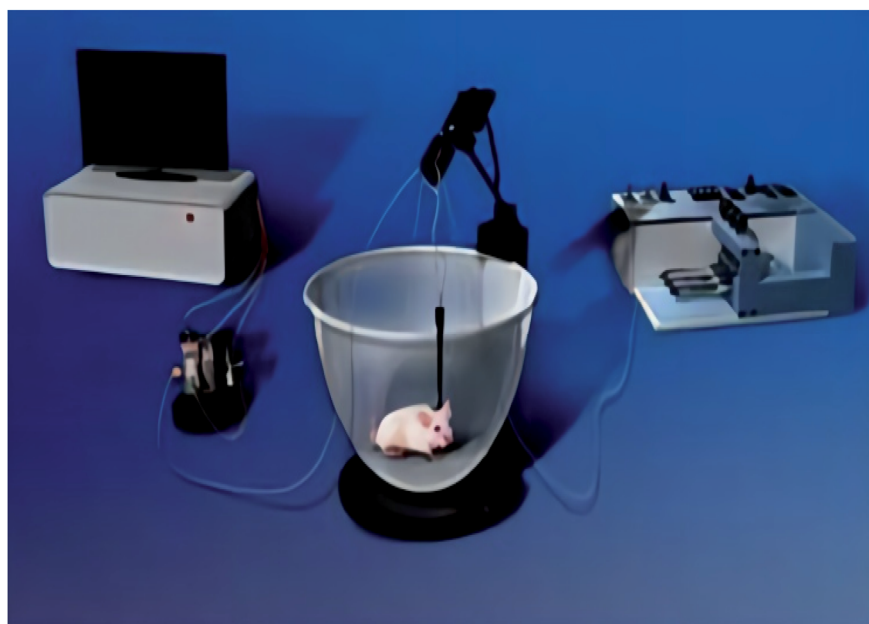
Since the amount of dialysis fluid is generally very small, the conventional macroelectrodes and electrochemical detection cell in this system is usually replaced by a thin-layer electrochemical flow-through cell (TEFC).<sup>21</sup> In the TEFC, the small volume (microliter level) of dialysate is restricted to a thin layer (2–100  $\mu\text{mol L}^{-1}$ ) on the electrode surface, thus the ratio of the electrode area and the volume of solution can be improved to achieve overall electrolysis conditions.

For example, Meining Zhang *et al.* Based on the principles of *in vivo* microdialysis sampling and radial TEFC,<sup>21</sup> they developed a new analytical system with single-walled carbon nanotube (SWNT) modified glassy carbon electrode (GCE) as the working electrode. The system can continuously monitor the ascorbic acid in rat striatum caused by systemic ischemia. It can be seen from Fig. 2 that the main structure of radial TEFC is a thin radial flow block. The sensor uses Ag/AgCl electrode (3 M NaCl) as the reference electrode, heat-treated SWNT modified GCE (diameter 6 mm) as the working electrode and stainless steel as the counter electrode. The thickness of the gasket used for this sensor is 50  $\mu\text{m}$ . The brain dialysate or standard solution is delivered through an airless syringe (BAS), and then pumped into the radial flow cell through a tetrafluoroethylene hexafluoropropylene (FEP) tube by a microinjection pump (CMA 100, CMA microdialysis AB, Stockholm, Sweden).

Generally, we need to replace different working electrodes to detect different substances. Ma *et al.* An integrated electrochemical biosensor based on dehydrogenase was constructed by using zeolite imidazole ester skeleton (ZIF) as matrix, which can be used to detect glucose content *in vivo*.<sup>26</sup> In order to verify the application of the sensor in electrochemical measurement *in vivo*, the glucose in microdialysate continuously sampled from guinea pig brain was monitored online by placing the biosensor of ZIF-70 in radial TEFC. In this case, the ZIF-70 biosensor is mainly obtained by dropping MG/MG/ZIF-70 dispersion on the modified GCE, then washing the electrode with water, and finally drying it. The system uses 50  $\mu\text{m}$ . The thin radial flow block of M gasket forms the flow cell. At the



A.



B.

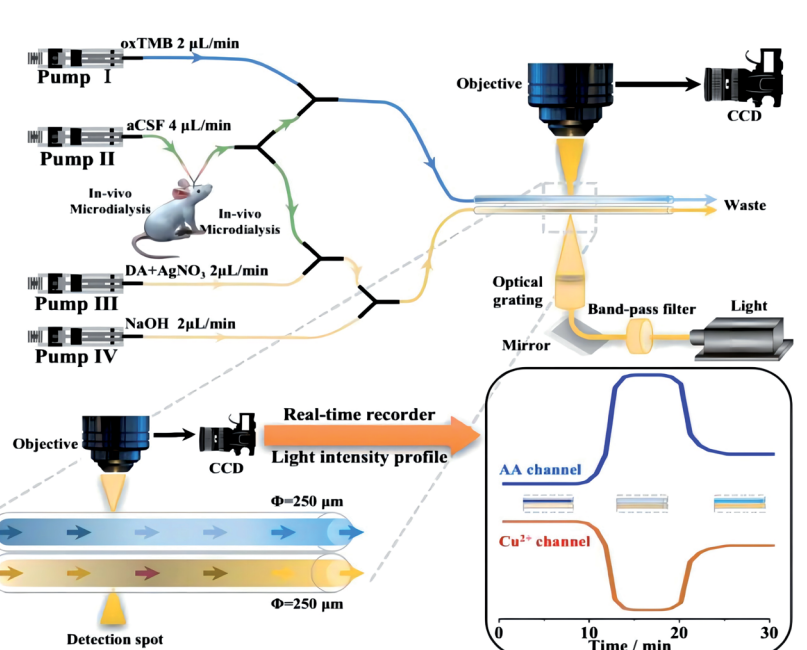


Fig. 1 Picture (A) is the on-line electrochemical detection system for *in vivo* monitoring combined with *in vivo* microdialysis in the past. Figure from Xulin Lu *et al.*<sup>22</sup> Reproduced with permission from *Anal. Chem.*, 2013, 85. Copyright American Chemical Society (2013). Picture (B) is the combination of microdialysis sampling and two colorimetric sensors to continuously and simultaneously monitor AA and Cu<sup>2+</sup> in the brain of living rats. Figure from Chao Wang *et al.*<sup>125</sup> Reproduced with permission from *Anal. Chem.*, 2021, 91. Copyright American Chemical Society (2021).

same time, Ag/AgCl electrode (3.0 M NaCl) is used as the reference electrode, the biosensor of ZIF-70 is used as the working electrode and stainless steel is used as the auxiliary electrode. Compared with other types of sensors, ZIF based biosensors have the advantages of high selectivity and high

sensitivity for the detection of glucose in the brain. Therefore, using ZIF as matrix co immobilized biosensors (including electrocatalysts and enzymes) is widely considered as a general method for the development of new electrochemical biosensors.

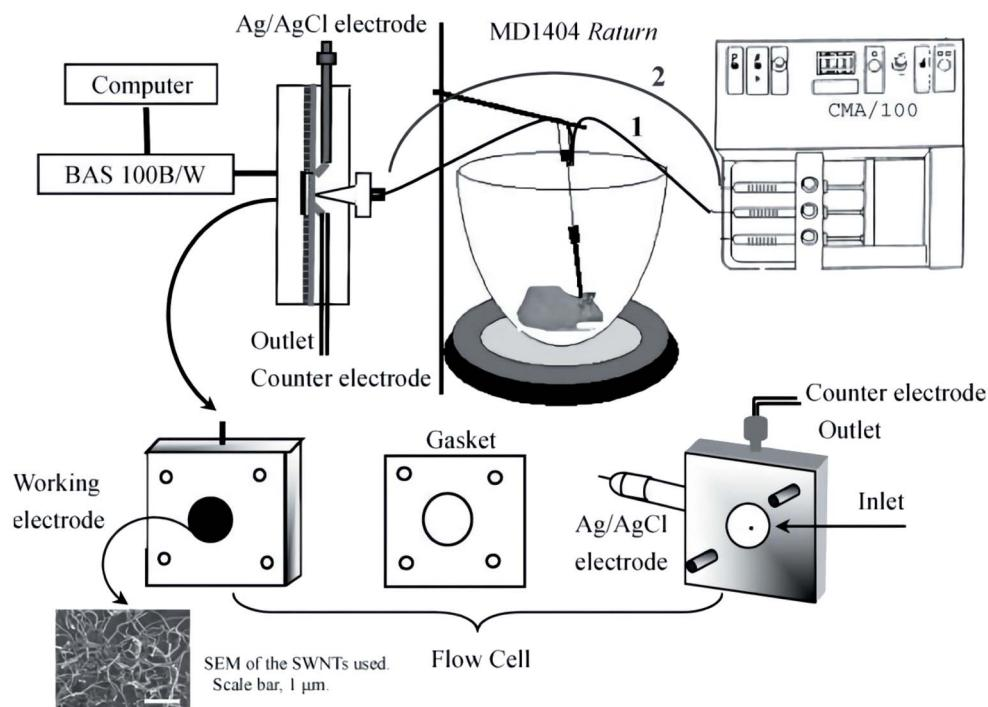
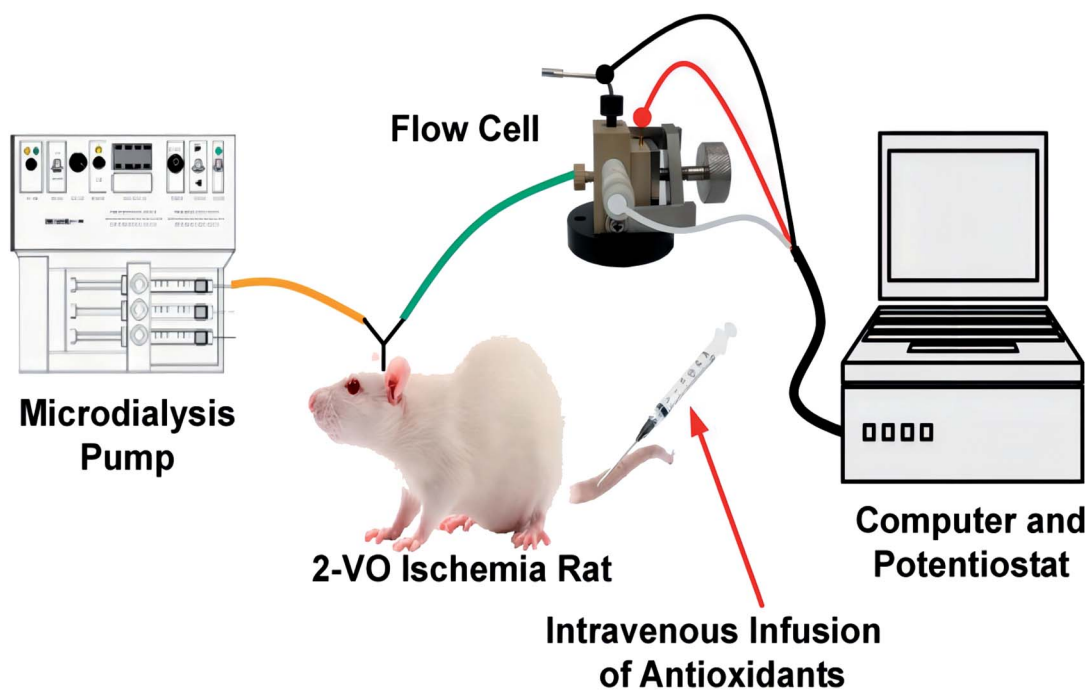
**A.****B.**

Fig. 2 Picture (A) the structure of thin layer electrochemical flow cell a for on-line measurements of the brain dialysate, the aCSF used as the perfusion solution is delivered from the syringe and pumped through the rat brain to the radial flow cell (line 1). The increase in the current response obtained in the text is then due to the oxidation of ascorbate in the brain dialysate with reference to the baseline recorded with pure aCSF that is also delivered from the syringes but pumped directly to the radial flow cell (line 2). For on-line evaluating the reproducibility of the electrode with the brain dialysate, lines 1 and 2 are alternatively connected to the electrochemical flow cell to obtain the current responses for ascorbate in the same brain dialysates several times. These steps additionally make it possible to evaluate the electrode reproducibility with the brain dialysate. Figure from Meining Zhang *et al.*<sup>21</sup> Reproduced with permission from *Anal. Chem.*, 2005, 77. Copyright American Chemical Society (2005). Picture (B) the detector is composed of a thin-layer electrochemical flow cell integrated with *in vivo* microdialysis. Used to detect ascorbic acid in rat brain, figure from Kun Liu *et al.*<sup>126</sup>. Reproduced with permission from *Anal. Chem.*, 2013, 85. Copyright American Chemical Society (2013).



By using this platform, Xulin Lu *et al.*<sup>22</sup> demonstrated a highly selective and sensitive three-dimensional conductive framework for *in vivo* microdialysis and electrochemical detection. This three-dimensional conductive framework is based on the hybridization of single wall carbon nanotubes (SWNT) and infinite coordination polymer (ICP) nanoparticles with bio-electrochemical activity. ICP nanoparticles with bio-electrochemical activity can be synthesized during the self-assembly of NAD<sup>+</sup> (nicotinamide adenine dinucleotide (oxidized state)) and Tb<sup>3+</sup> (terbium ion), and all biosensor elements including cofactors *i.e.* β-nicotinamide adenine dinucleotide, NAD<sup>+</sup>, enzyme (*i.e.* glucose dehydrogenase, GDH) and electrocatalyst (*i.e.* methylene green, Mg) are adaptively encapsulated. ICP/SWNT nanocomposites can be used to simply prepare ICP/SWNT based biosensors on glass carbon substrates. This sensor shows great advantages over ICP biosensors prepared by ICP nanoparticles (*i.e.* no SWNT hybridization). It has higher sensitivity and stability in electrochemical research. Because almost all the effective electrons of the ICP limited to the electrode can be transmitted by SWNT, and even if they are far away from the electrode, the ICP can easily find the nearby wires. The electrochemical biosensor based on GDH is a good example. Combined with *in vivo* microdialysis, the biosensor of ICP/SWNT is used as an on-line detector in continuous flow system to build a simple but effective on-line electrical analysis platform for continuous monitoring of glucose in guinea pig brain. This study simplifies the preparation of biosensors and is considered.

To sum up, with the application of new matrix materials and the high selective enzyme, the modified working electrodes fixed in the thin-layer electrochemical flow cells have achieved good results in terms of single component *in vivo* measurements. However, in the simultaneous measurement of multiple components, the MD-thin layer electrochemical flow cell system has not done well. Because of the restrictions on the structure of thin layer electrochemical flow cell, it is difficult to increase the working electrode surface, furthermore, it is difficult to find an enzyme which can measure two or more substances with high selectivity and accuracy.

## 2.2 MD-electrochemical microfluidic chip *in vivo* detection system

To solve the problem of multi-component measurements, Hoang-Thanh Nguyen *et al.* directly integrated electrochemical flow cell based on microfluidic chip combined with the micro dialysis to continuously and simultaneously monitor the multiple chemicals in living bodies.<sup>122</sup>

Miniaturization and integration are important developing directions to modern analytical chemistry.<sup>35</sup> Micro-electromechanical systems (MEMS) provide the convenient conditions for the miniaturization development of analytical instruments. In the early 1990s, Manz and Widmer *et al.* first presented MEMS-based miniaturized total analysis system (μTAS).<sup>36</sup> The μTAS integrated the laboratory analytical functionalities (including sampling, diluting, adding reagents, mixing, reaction, separation, detection, *etc.*) into a portable

device, or into a few square centimeters chip. The progress of the micro-processing technology promote the miniaturization of μTAS. Various function components like micro-channels, micro-valves and micro-reservoirs, microelectrodes, and connectors, *etc.* can be manufactured on the microchip. Now electrochemical measurements is the method which can achieve the microfluidic detection on a chip.

Woolley *et al.* 1998 reported the first case of microchip capillary electrophoresis amperometric detector<sup>37</sup> Subsequently, the reports on the electrochemical detection on microfluidic chips gradually increased.<sup>38,39</sup> Graß *et al.* made a detailed description of the production of isotachophoresis – conductivity chip detector on the substrate.<sup>40</sup> Prest *et al.* design a special contacting single-electrode conductivity detector for the separation and analysis of chip isotachophoresis.<sup>41,42</sup> Chaoxiong Ma *et al.* Recessed ring disk (RRD) electrode arrays with nano-pitch are fabricated by nanosphere lithography, multilayer deposition and multi-step reactive ion etching techniques and incorporated into nanofluidic channels, making these arrays characteristic in nanofluidic channels be displayed, that is (Fig. 3), the redox cycle leads to current amplification during cyclic voltammetry (CV) redox reversibility or redox potential enables electroactive substances to be selectively analyzed.<sup>43</sup>

In the same year, Chaoxiong Ma and co-workers found the recessed disk array electrodes which had been constructed suitable to do the detection of pyrocatechol and dopamine in the presence of interferences. This study shows that reducing the electrode spacing and size to nano scale can further improve the sensor performance (Fig. 4), and proves some advanced advantages of ring disk geometry.<sup>44</sup>

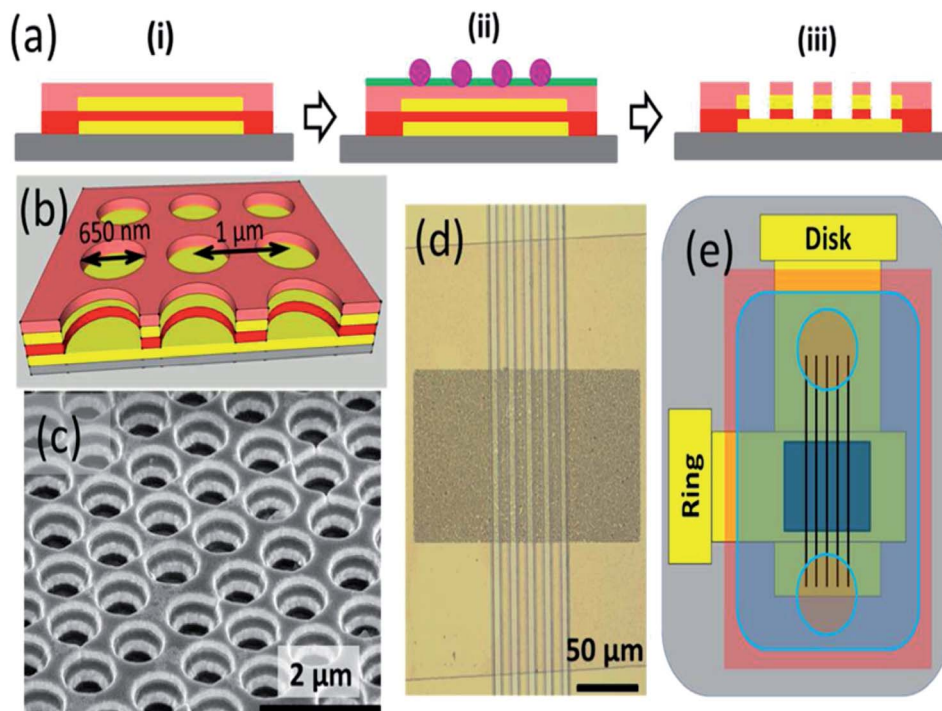
Jae Hyoung Park *et al.* designed a polydimethylsiloxane (PDMS) microfluidic chamber with microsieves, and they immobilized high-density photosynthetic cells in a monolayer, allowing it to measure measurements with two internal metal electrodes photosynthetic activity of cells. PDMS microfluidic chamber is fabricated by soft lithography with two electrodes connected to glass substrate by sputtering method. The microfluidic chamber was manufactured, and the characteristics of internal electrodes in redox solution were measured by CV. In PDMS microfluidic chamber, dense cells were accumulated in hydrogel or water environment. Meanwhile, the physiological characteristics of cell photosynthesis could be analyzed by potentiometry or current method. The generation rate and oxygen distribution in cell photosynthesis process could also be simulated to estimate<sup>45</sup> quantitatively (Table 1).

Although the above experiments have not been performed *in vivo*, these experiments provide a good foundation for future applications of *in vivo* assays.

Jiang Liu *et al.* have been conducting research in the area of *in vivo* multi-component detection through a MD-electrochemical microfluidic chip and have made some progress.<sup>123</sup> An on-line electrochemical detection system based on microfluidic chip was developed by Xia Gao *et al.*<sup>47</sup> The detection system can realize the continuous online real-time detection of ascorbic acid and Mg<sup>2+</sup> in rat brain. The microfluidic chip is used as the detector of two species in the system. The detector is made by combining the



A.



B.

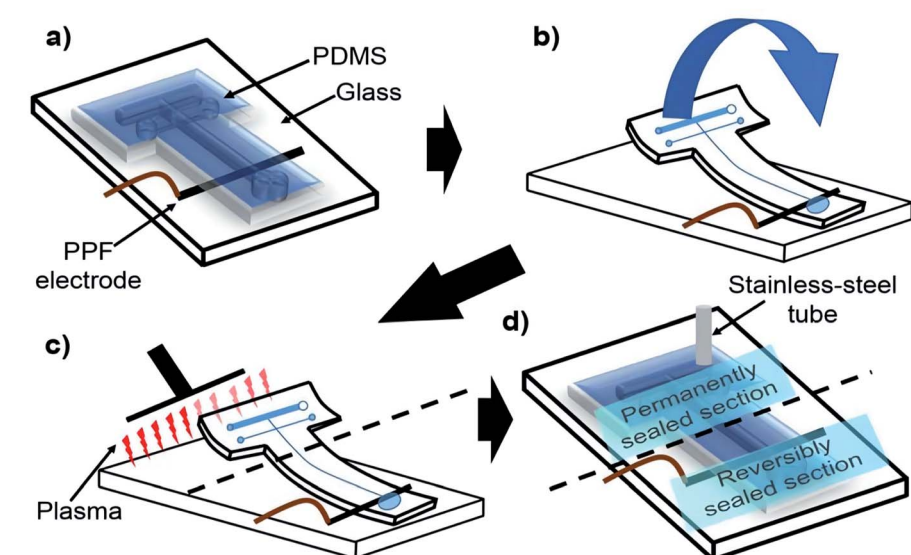


**Fig. 3** (A): (a) Schematic cross section showing the fabrication procedure for the RRD array, including (i) layer-by-layer deposition, (ii) nano-sphere lithography, and (iii) multistep reactive ion etching. The colors represent different layers: gray (glass slide), yellow (Au), red ( $\text{SiN}_x$ ), pink ( $\text{SiO}_2$ ), purple (polystyrene spheres), and green (Cr). (b) Schematic diagram of the ring-disk geometry of the array. (c) An SEM image of the array at 50° tilt. (d) An optical image of the array integrated with  $\text{SiN}_x$  channels. (e) Schematic diagram of the macroscopic layout of the RRD array (dark blue) integrated with channels (black) and covered by a piece of PDMS (light blue) with two circular wells. Figure from Chaoxiong Ma *et al.*<sup>43</sup> Reproduced with permission from *Anal. Chem.*, 2013, 85. Copyright American Chemical Society (2013). (B) Improved chip bonding procedure: (a) reversibly align the microchannel with the PPF electrode, (b) fold back the top section of the chip from the glass and temporarily tape to the opposite end of the glass plate, (c) simultaneously expose the top sections of the PDMS chip and the glass substrate, (d) re-seal the chip onto substrate by removing the tape and insert a stainless-steel tube to connect the chip to MD flow. Reproduced with permission from *Anal. Chem.*, 2020, 145. Copyright American Chemical Society (2020).



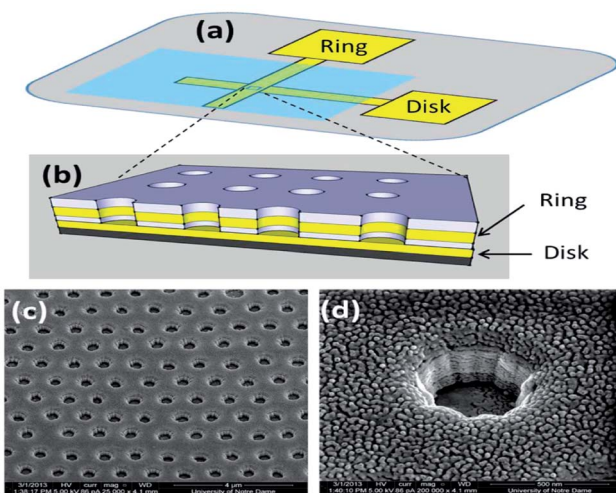


Fig. 4 (a) Schematic diagram showing the macroscopic layout of the device and (b) ring-disk geometry in the nanopores. (c) SEM image of the array at 52° tilt; (d) magnified view for a single electrode at 52° tilt. Figure from Chaoxiong Ma *et al.*<sup>44</sup> Reproduced with permission from ACS nano, 2013, 7. Copyright American Chemical Society (2013).

stainless steel tube with the Ag/AgCl line as the reference electrode, developing the single channel microfluidic chip into an electrochemical flow cell as the counter electrode, and combining the chip with the indium tin oxide (ITO) electrode as the working electrode. In order to realize the selective detection of ascorbate and  $Mg^{2+}$  (Fig. 5), toluidine blue (polytbo) film and single wall carbon nanotube (SWNT) were coated and polymerized on ITO electrode at the same time. In addition, in order to avoid any crosstalk between the two electrodes, the solution introduction mode and arrangement of polytbo modified electrode and SWNT modified electrode were carefully designed. By directly integrating the electrochemical flow cell based on microfluidic chip with *in vivo* microdialysis, and using the electrochemical flow cell of microfluidic chip as a detector, an online electrochemical detection system can be successfully established. The detection of  $Mg^{2+}$  and ascorbic acid by microfluidic system can show a good linear relationship respectively. In addition, the system shows good reproducibility, high stability and high selectivity for the detection of these two substances in a continuous flow system.

It was because of the unmatched advantages microfluidic chips system has in contrast to those traditional macro-scale instruments, the multi-working electrode exist on the a few square centimeters chip without any cross talk and could continuously and simultaneously detect multiple chemical components. And the system was expected to make a greater contribution to the *in vivo* analysis in the future (Table 2).

However, in this platform, dialysate samples needed to get through a long tubing before they reached the detector cell, and there was bound to affect the real-time detection, and limited the scope of the experimental animals activities. It was extremely uncomfortable to the animals anesthetized or fixed on the stereotaxic apparatus throughout the test, and the recording processes are not natural.

Moreover the main disadvantage of microdialysis electrochemical sensing platform was the high cost of microdialysis probe, and the dialysis membrane could be blocked by proteins and other macromolecules easily, thus the membrane was difficult to be reused.

### 3. Microelectrode (ME)-electrochemical *in vivo* detection system

Facing such drawbacks of microdialysis-electrochemical sensing systems, Shaneelchandra *et al.*<sup>15</sup> designed microelectrodes by modifying the materials or components of the electrodes to achieve *in situ* analysis of *in vivo* targets, which can directly improve the sensitivity, thermal stability, and anti-contamination of the electrodes. For example, by changing the inherent properties of the electrode itself, such as BDD and other electrode materials, the robustness and anti-pollution properties of the electrode can be significantly improved. Of course, it can also be coated with a layer of anti-pollution material, such as Nafion, on the surface of the electrode to resist biofouling. Finally, it can also reduce pollution through electrode hydrogenation technology.

#### 3.1 The carbon fiber microelectrode (CFME)

Carbon fiber microelectrodes (CFMEs) have good biocompatibility, easy insertion, and electrode diameters as small as 10  $\mu$ m, making *in vivo* electrochemical detection more reliable.<sup>128</sup>

**3.1.1 CFME classical electric wire-connected electrochemical *in vivo* measurements on animals.** The bioactive substances in animals are detected by the combination of CFME and electrochemical detector, *in vivo* studies mainly take rats and mice as model organisms to determine the functional effects of these substances, because they have the advantages of short growth cycle, easy operation and fast reproduction.

However, *in situ* analysis and accurate detection in complex animal tissues are very difficult, and more efforts are required to construct high-performance biosensors for real-time *in situ* detection *in vivo*.<sup>137</sup> Interestingly, a bovine erythrocyte copper zinc superoxide dismutase (sod-e2zn2sod) was designed by Chai Xiaolan *et al.*,<sup>10</sup> E designates an empty site functionalized CFME which combined with a 6-(ferrocenyl) hexanethiol (FcHT)-modified CFME for high selectively and accurately detecting  $Cu^{2+}$  ions in rat brain. Simultaneously, they synthesized a gold-truncated octahedral microcapsule filled with nanoparticles, which exhibits high electrocatalytic activity and large surface area for significantly improved sensitivity. In addition, the concentration estimated by ICP-AES method is highly consistent with the concentration of  $Cu^{2+}$  in rat brain measured by this sensor.

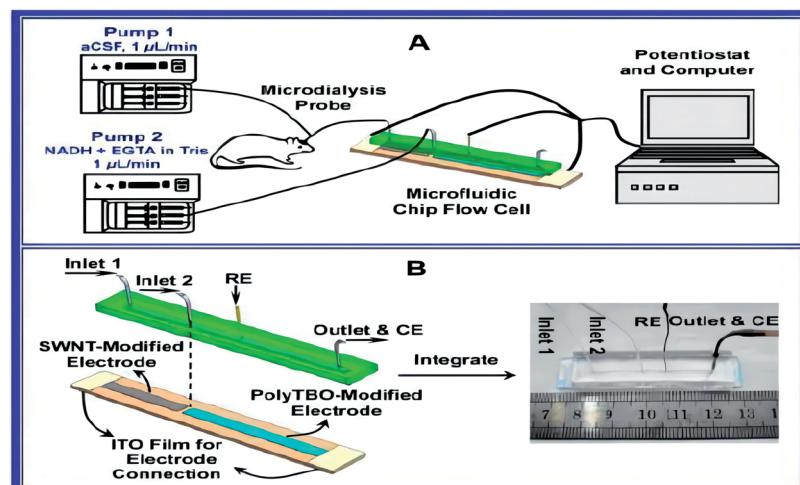
Although  $Cu^{2+}$  level in rat brain can be monitored by dual channel ratio electrochemical biosensor, in order to achieve continuous monitoring, the important problem of long-term stability of implantable microelectrode must be considered. The original sensitivity of the sensor will be reduced or even lost because a large amount of albumin and other circulating



Table 1 Properties of on-line MD-thin-layer electrochemical flow cell electrochemical sensors for *in vivo* measurement

Working electrodes	Enzymes	Experimental model	Dialysis site	Analytes	Dynamic linear range	Detection limit	Ref.
Heat-treated SWNT-modified GC electrode		Adult male sprague dawley rats (350–400 g)	Striatum	Ascorbate	0.50 to 100 $\mu\text{mol L}^{-1}$	0.20 $\mu\text{mol L}^{-1}$	21
GOD-Pin/MWNT-modified GC electrodes	GOD	Adult male guinea pigs (300–400 g)	Striatum	Glucose	300 to 1500 $\mu\text{mol L}^{-1}$		28
polyTBO-Modified GC electrode		Male guinea pigs (260–320 g)	The left side of the brain	$\text{Mg}^{2+}$	0.05 to 2.0 $\text{mmol L}^{-1}$		33
GDH-MG/ZIF-70-modified GC electrodes	GDH	Adult male guinea pigs (300–400 g)	Striatum	Glucose	0.1 to 2 $\text{mmol L}^{-1}$		26
ICP/SWNT-modified GC electrodes		Adult male guinea pigs (300–400 g)	Striatum	Glucose	50 to 1000 $\mu\text{mol L}^{-1}$		22
SWNT-modified GC electrode		Adult male sprague dawley rats (300 $\pm$ 50 g)	Dorsal hippocampal	Ascorbate	0.5 $\mu\text{mol L}^{-1}$ to 100 $\mu\text{mol L}^{-1}$		27
GlutaOx-[C <sub>3</sub> (OH) <sub>2</sub> min][BF <sub>4</sub> ]-Au/Pt-nafion GC electrode	GlutaOx	Rat	Striatum	Glutamate	0.5 $\mu\text{mol L}^{-1}$ to 20 $\mu\text{mol L}^{-1}$	0.17 $\mu\text{mol L}^{-1}$	31
{IL-RGO/S-RGO <sub>n</sub> /GOx/nafion GC electrode	GOx	Male sprague dawley rats (weight ranges from 200 to 250 g)	Striatum	Glucose	10 $\mu\text{mol L}^{-1}$ to 500 $\mu\text{mol L}^{-1}$	3.33 $\mu\text{mol L}^{-1}$	29
GlutaOx/MWCNTs/PAMAM/Pt-nafion biosensor or SWNT-modified glassy carbon working electrode (6 mm diameter)	GlutaOx	Male sprague dawley rats (weight ranges from 200 to 250 g)	Striatum	Glutamate	1.0 $\mu\text{mol L}^{-1}$ to 50.0 $\mu\text{mol L}^{-1}$	0.5 $\mu\text{mol L}^{-1}$	30
Carbon pyrolyzed photoresist film electrode		Adult male sprague dawley rats (3 months of age, 300 $\pm$ 50 g)	Right side of the olfactory bulb and right side of the caudoputamen	Ascorbate	5 $\mu\text{mol L}^{-1}$ to 100 $\mu\text{mol L}^{-1}$		34
Carbon fiber microelectrodes		Sprague dawley rats (weight ranges from 250 to 400 g)	Striatum	Catecholamines			98
Functionalized gold electrodes (Au, 2 mmol L <sup>-1</sup> in diameter)		Freely roaming sheep		Adenosine	25 $\mu\text{mol L}^{-1}$	99	
Graphene oxide (GO) modified electrode	AA oxidase (AOX)	Male sprague dawley rats (250–300 g, Brain 6–8 weeks)	Brain cortex	ATP	0.1 nmol L <sup>-1</sup> to 1 mmol L <sup>-1</sup>	50 pmol L <sup>-1</sup>	100
Cu <sup>2+</sup> /Cys/Au electrode		Adult male sprague dawley rats	Ventral hippocampus	Ascorbic acid	0.5 $\mu\text{mol L}^{-1}$ to 1000 $\mu\text{mol L}^{-1}$	10 nmol L <sup>-1</sup>	101
PtNPs nanocomposite ink		Male sprague dawley rats (200–400 g)	Gray matter of the spinal cord	H <sub>2</sub> S	0.01 $\mu\text{mol L}^{-1}$ to 100 $\mu\text{mol L}^{-1}$	5 nmol L <sup>-1</sup>	102
Ag/AgCl electrode (0.6 mm, in diameter) was inserted into the glass capillary	Glutamate oxidase	Adult male sprague dawley rats (250–300 g)	Brain cortex	Glutamate	1 $\mu\text{mol L}^{-1}$ and 800 $\mu\text{mol L}^{-1}$	0.5 $\mu\text{mol L}^{-1}$	103
				ATP	5 nmol L <sup>-1</sup> to 100 nmol L <sup>-1</sup>		104

A.



B.

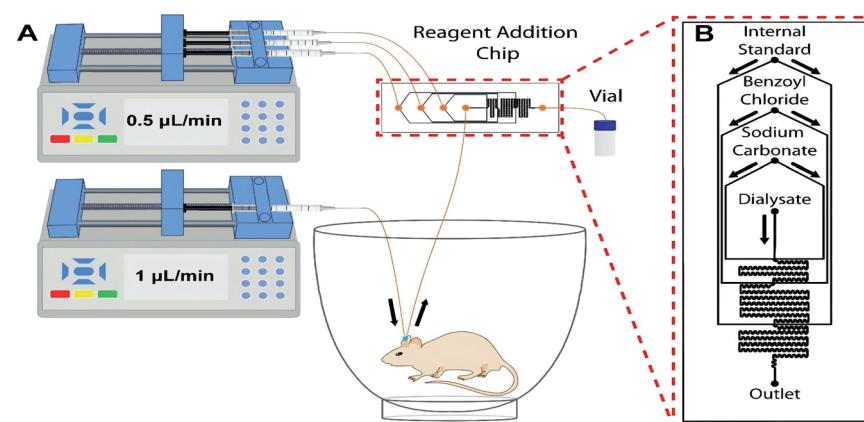


**Fig. 5** (A) Scheme (A) Schematic illustration of the microfluidic chip-based online detecting system for continuous and simultaneous monitoring of ascorbate and  $Mg^{2+}$  in rat brain and (B) structure of the microfluidic chip-based electrochemical detector. The microfluidic chip-based detector consists of two independent substrates: upper wafer, PDMS chip with a channel as a continuous flow microfluidic cell, 40 mm in length, 1 mm in width, and 500  $\mu$ m micrometer in depth; lower wafer, SWNT-modified and poly TBO modified electrodes as dual working electrodes. Ag/AgCl wire and stainless steel tube (also as outlet) were separately embedded into the PDMS chip and used as reference electrode (RE) and counter electrode (CE), respectively, for the electrochemical detection. Figure from Yuqing Lin *et al.*<sup>46</sup>. Reproduced with permission from *Anal. Chem.*, 2013, 25. Copyright American Chemical Society (2013). (B) An illustration of an experimental setup for microdialysis sampling coupled with on-chip BzCl derivatization in awake animals. Figure from Alec C. Valenta *et al.*<sup>127</sup>. Reproduced with permission from *Anal. Chem.*, 2021, 146. Copyright American Chemical Society (2021).

proteins in cerebrospinal fluid pollute the sensor surface, and this might be the reason why this approach was only a point in time detection of  $Cu^{2+}$  ions, not a continuous monitoring in rat brain. It was the same as some other recent researches *e.g.* in the work of Ste'phane Fierro *et al.*<sup>49</sup> to obtain reliable results, the *in vivo* current measurement should not last more than 5 s.

Electrochemical measurement has been widely used for *in vivo* measurement of electroactive biological events in model systems (such as rats, mice and primates). However, in recent years, electrochemical monitoring of small model animals such as fruit flies is still not feasible.<sup>50-52</sup>

The change of extracellular monoamine concentration in the ventral nerve cord of a single drosophila larva was measured in

real time by Xenia Borue and colleagues<sup>53</sup> for the first time. Using fast scanning cyclic voltammetry (FSCV) on implanted microelectrode (CFME), channel rhodopsin-2-mediated neuron type specific stimulation can be detected to trigger endogenous serotonin release. They confirmed that the substance tested was serotonin by reducing the release after pharmacological inhibition during serotonin packaging or synthesis. The concentration of serotonin induced in flies is similar to that induced by tetanus in mammals, with a concentration of 280–640 nmol  $L^{-1}$ . The specific concentration depends on the stimulation length. After fluoxetine or cocaine is given, the extracellular serotonin signal in the detector is significantly prolonged, indicating that serotonin is cleared during the regulation of

Table 2 Properties of on-line MD-thin-layer electrochemical microfluidic chip for *in vivo* measurement

Working electrodes	Enzymes	Experimental model	Dialysis site	Analytes	Dynamic linear range	Detection limit	Linear efficiency	Ref.
SW/NT-modified ITO electrode		Adult male sprague dawley rats (250–300 g)	Striatum	Ascorbate	1 to 50 mmol L <sup>-1</sup>	0.50 $\mu$ mol L <sup>-1</sup>	0.999	46
SW/NT-modified electrode poly/TBO-modified electrode		Adult male sprague dawley rats (250–300 g)	Striatum	Ascorbate Mg <sup>2+</sup>	5 to 100 $\mu$ mol L <sup>-1</sup> , 100 to 2000 $\mu$ mol L <sup>-1</sup>	0.9999, 0.9987	47	
(Polypyrrole (PPy)-protected) thin-film Pt electrode	GOx	Male wistar rats (350–410 g)	A deep subcutaneous tissue layer	Glucose	2.1–20.6 mmol L <sup>-1</sup>	0.997	48	
3D nanoporous Au–Ag alloy microwire (NPAMW) modified with MIP works		Healthy rabbit	Venous blood	WFS	5–400 $\mu$ mol L <sup>-1</sup>	2 $\mu$ mol L <sup>-1</sup>	0.997	105
Pyrolyzed photoresist film electrode		Male sprague dawley rats (250–300 g)	Striatum	Dopamine		1 $\mu$ mol L <sup>-1</sup>		106
CMOS biosensor microchip		Male and female adult mice (8 to 12 weeks)	Adrenal tissue	Catecholamine	8–1024 $\mu$ mol L <sup>-1</sup>	15.7 $\mu$ mol L <sup>-1</sup>	0.9913	107
Cylindrical flexible enzyme-electrode sensor	GOx	Healthy sprague dawley rats	Subcutaneous tissue of the rat's posterior neck	Glucose	0–570 mg dL <sup>-1</sup>	3.54 mg dL <sup>-1</sup>		108

extracellular transport. The sensor can target dopaminergic neurons through ChR2 to measure the release of dopamine *in vivo*, which indicates that the detection of other neurotransmitter systems can also be determined by this method. In this study, they found that the dynamics of serotonin release and reuptake in *drosophila* is highly similar to that in mammals, so a simple model animal like this is very effective for studying the basic physiological mechanism of serotonin. Monique A. Makos *et al.* designed a background reduced FSCV method to monitor dopamine in *drosophila* CNS using CFME.<sup>54</sup> Absorption of exogenous dopamine by dopamine transporter (DAT) in adult *drosophila*. Monique A. Makos *et al.* Verified the model system for studying the mechanism of drug addiction by comparing the dopamine concentration of fuming (FMN) mutant *drosophila* and wild-type *drosophila* before and after cocaine (which is known to prevent data from absorbing dopamine) treatment.

After the applicability of *D. melanogaster* larva model was demonstrated, the work in recent years involved using larva to test the biological practicability of modified electrode.<sup>55</sup>

ChR2 mediated serotonin release in the ventral nerve cord of *Drosophila melanogaster* larvae can be measured by COOH–CNT, modified disk electrode and carboxylic acid carbon. The electrode was fabricated by modifying carbon fiber disk micro-electrode with carboxylic acid functionalized carbon nanotubes, and then immersed in carbon nanotube suspension. The sensitivity of serotonin measured with COOH–CNT electrode is 2.5 times higher than that of pure carbon fiber electrode, and the electrode can remain stable for several h.

In addition to these brain microelectrode analyses, there were some other parts *in vivo* biological events analyses have made some achievements.

Liu Junxiu *et al.*<sup>56</sup> designed an *in vivo* method for real-time monitoring the changes of ascorbic acid level in cochlear extralymphatic lymph of guinea pigs in the acute stage of tinnitus to study the role of ascorbic acid in the pathological process of tinnitus. They induced the acute stage of tinnitus by modifying CFME with multi walled carbon nanotubes (MWNT) and microlocal input of salicylate. In order to continuously detect ascorbic acid in cochlear extralymphatic microenvironment in real time, they used micro Ag/AgCl as reference electrode, Pt line as counter electrode and MWNT modified CFME as working electrode. At the same time, the three electrodes are combined around the capillary to form an integrated capillary electrode, and then the integrated electrode is carefully implanted in the cochlear lymph of guinea pigs. Finally, a small amount of salicylate is injected into the cochlear lymph to realize the real-time monitoring of ascorbic acid level. In this study, this integrated capillary electrode has good linearity and high selectivity for the determination of ascorbic acid. This study provides a new strategy for the *in vivo* monitoring of ascorbic acid in cochlear extralymphatic lymph after salicylate induced tinnitus, so it can be used for the physiological characteristics related to tinnitus.

Since almost no clinical diagnosis of the brain diseases need to do the examination by a implantable probe, and similarly, subcutaneous glucose monitoring is considered much more

practical than the cerebral glucose monitoring. Because we have too little research on the measurement of peripheral tissues, the clinical application of electrochemical sensors has stopped at blood glucose meters, and there has been no major progress. This may also be caused by our over-research on biosensors in the brain.

**3.1.2 CFME classical electric wire-connected electrochemical *in vivo* measurements on plants.** Compared to the above electroanalytical methods for *in vivo* measurements on animals, a hemoglobin (Hb) – modified carbon fiber ultra-microelectrode (CFUME) and single wall carbon nanotubes (SWCNTs) were designed by Qiong-Qiong Ren and his colleagues<sup>45</sup> to monitor the oxidation burst of aloe. Through this method, an *in vivo* H<sub>2</sub>O<sub>2</sub> sensor with direct electron transfer can be constructed. Hb/SWCNTs/CFUME can directly monitor H<sub>2</sub>O<sub>2</sub> in aloe leaves under salt stress *in vivo* within 19.5 h by taking advantage of low working potential and small size, and this method does not need additional surface coating and complex data processing to avoid interference (Fig. 6). Although both are *in vivo* tests, the effective monitoring time of micro-electrodes in animals and plants is very different. Therefore, we infer that the albumin and other circulating adhesion

substances in plants are not less than that in animals. This requires us to find the reason.

**3.1.3 CFME wireless electrochemical *in vivo* measurements on animals.** Additionally, there is another great difference between plants and animals *in vivo* detection. Although no microdialysis probe and long tubings in the micro-electrodes electrochemical *in vivo* detection system, the microelectrode still need wires to connect with the electrochemical workstation, thus the animals must be anesthetized or be fixed on a stereotaxic apparatus. That is bound to increase the difficulty of the experiment, and affect the mood and physiological state of the experimental animals, and may interfere with the accuracy of the experiment. Therefore, changing the connection form of micro-electrodes and electrochemical workstations is very critical.

In 2010, the development of wireless *in vivo* voltammetry of neurotransmitters in freely behaving rats was described by Francesco Crespi.<sup>58</sup> In this case, unidirectional infrared (IR) based on direct current (DCA) or differential pulse voltammetry (DPV) is used to improve the “diffusion” of the transmission channel of the telemetry system. The system has the characteristics of small weight (only a few grams) and very small

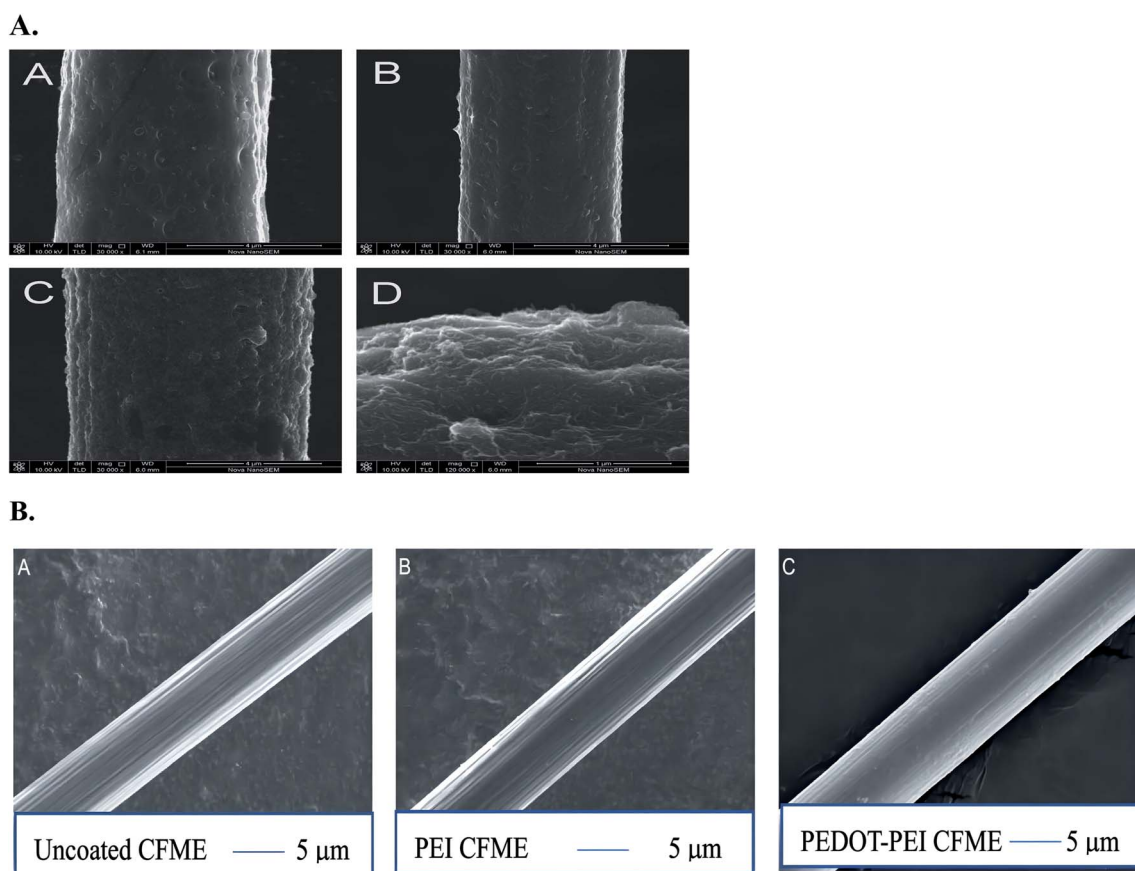


Fig. 6 (A) SEM images of bare CFUME (A), SWCNTs/CFUME (B), Hb/SWCNTs/CFUME (C) and tip of Hb/SWCNTs/CFUME(D). Figure from Qiong-Qiong Ren *et al.*<sup>57</sup> Reproduced with permission from *Biosensors and Bioelectronics*, 2013, 50. Copyright Elsevier Ltd (2013). (B) SEM images of (A) uncoated CFMEs approximately 7  $\mu\text{m L}^{-1}$  in diameter. (B) CFMEs electrodeposited with polyethylenimine (PEI). A thin layer of polymer evenly coats the surface of the electrode and fills the ridge of the fiber. (C) CFMEs electrodeposited with poly(3,4-ethylenedioxythiophene) (PEDOT)-PEI. Reproduced with permission from *Anal. Chem.*, 2020, 167. Copyright American Chemical Society (2020).



structure. But what is more interesting is that the system adopts one-way communication, which avoids the problems related to cross and changes the function of the measuring electrode system, this is the biggest difference from similar pre-existing instruments based on IR transmission.<sup>59</sup> In addition, it also has the advantage of electromagnetic interference free from interference RF transmission.

This study shows that the system seems to be highly sensitive to serotonin (5-HT) and dopamine (DA), whether using DPV or DCA, *in vivo* or *in vitro*. Especially after fluoxetine stimulated the 5-HT system in the frontal cortex of anesthetized rats, the use of wireless DCA or classical wired DCA in parallel *in vivo* tests in anesthetized rats resulted in data overlap.

In this Research, Francesco Crespi successfully applied a wireless method of biosensors to freely moving conscious rats, while Nafion was used in the prefrontal cortex® the 5-HT current related signals of the coated microbial sensor and the chemical properties of DA were specially pharmacologically verified (Fig. 7).

To sum up, the telemetry system has two great advantages: the first is that the sampling speed of biological substances (such as dopamine or serotonin) is fast, which can be sampled every 100 milliseconds. Secondly, its weight and size are very small, which can be effectively implanted into mice without affecting the movement of mice. This is considered to be a valuable feature of a telemetry system for real-time voltammetric monitoring of neurotransmitters.<sup>60</sup>

Currently, a self-powered skin patch electrochromic biosensor has been developed. This sensor can detect the concentration of lactic acid in the range of 0–10 mM by visually measuring the metabolites in sweat,<sup>129</sup> so animals do not need to be anesthetized. For example, humans can hide themselves and receive signals in another room to carry on direct *in situ* and realtime measurement of electronically active chemicals in freely behaving animals, and through a variety of emotional stimuli such as heating or giving an electric shock, man can observe if there have any changes of cerebral extracellular content of neurotransmitters, and can do some pharmacological

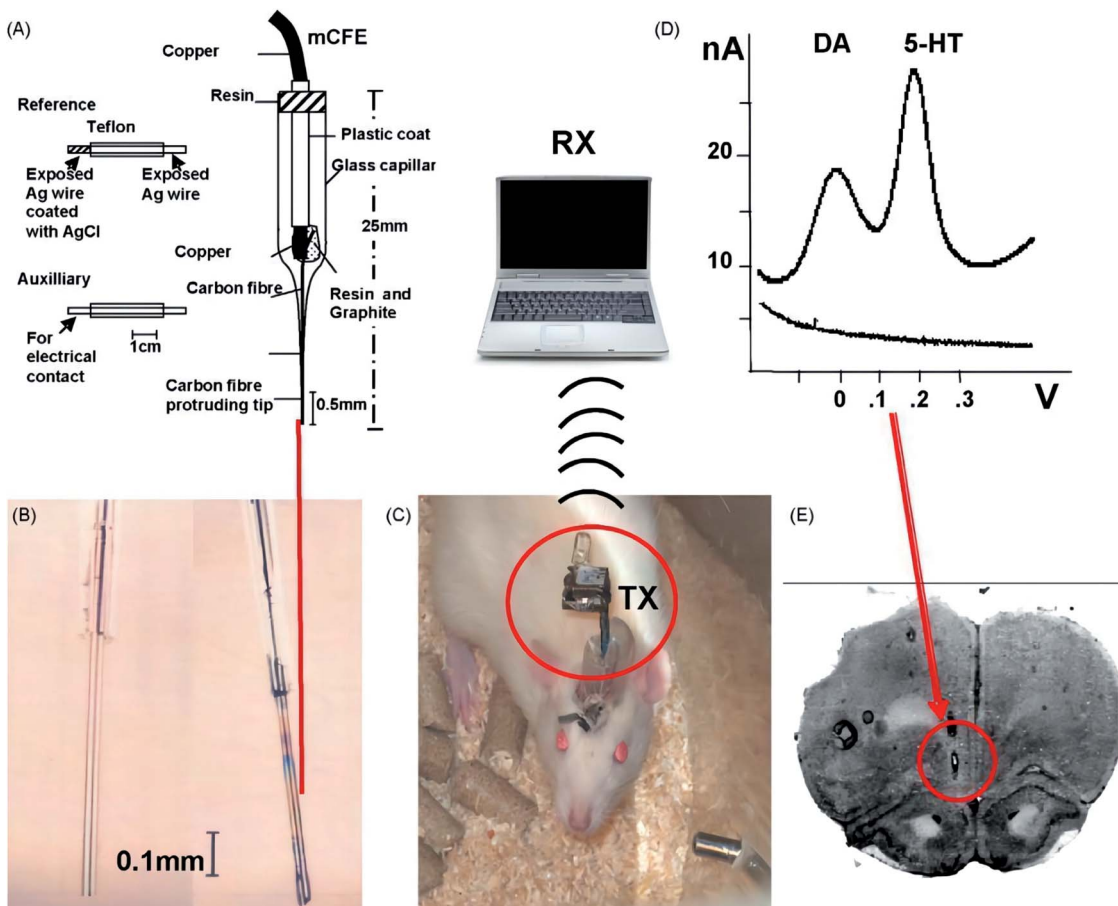


Fig. 7 (A) Drawing of auxiliary, reference and mCFE and details of construction. (B) Magnification of the electroactive tip of the mCFE before (left) and after Nafion® coating. (C) The behaving freely moving rat with TX placed upon its head that transmits the signal via an infrared channel to the receiving station (RX). A laptop computer, interfaced to the receiving station, performs the required signal acquisition and analysis. (D) Representative *in vitro* DPV curves for dopamine 5 M and serotonin 5 M in PBS (pH 7.4) as measured with Nafion®-mCFE (Crespi et al., 1988). *In vivo* studies, the tip of the Nafion®-mCFE is inserted in the rat prefrontal cortex as shown by the red arrow in (E) (for interpretation of the references to color in this figure legend, the reader is referred to the web version of the article). Figure from Francesco Crespi. Reproduced with permission from *Biosensors and Bioelectronics*, 2010, 25. Copyright Elsevier Ltd (2010).



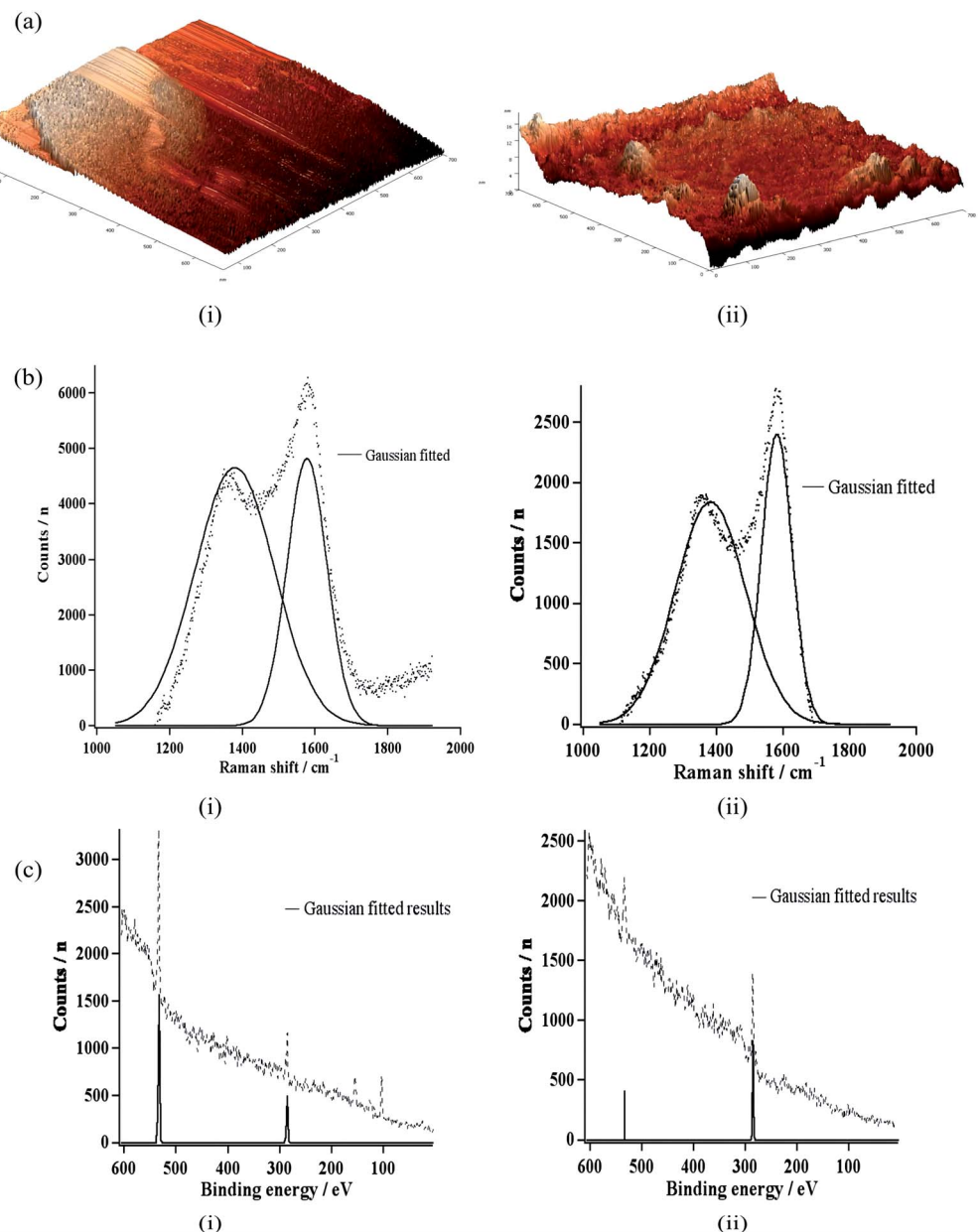


Fig. 8 (a) Atomic force micrographs, (b) Raman spectra, and (c) X-ray photoelectron spectra of (i) a bare carbon electrode and (ii) a hydrogenated carbon electrode. Figure from Shanel Chandra *et al.*<sup>15</sup> Reproduced with permission from *Anal. Chem.*, 2014, 86. Copyright American Chemical Society (2014).

experiments *etc*. However, how to further reduce the interference and ensure the accuracy in long term remote sensing *in vivo* experiments remains a problem need to be solved.

### 3.2 The glass substrates of conical-tip carbon electrodes

The lack of rigidity is also a big weakness of CFME. For the fabrication of *in vivo* targets-sensing microelectrodes, it is natural to consider the mechanical strength. In this regard, other materials *e.g.* the glass substrates of conical-tip carbon,<sup>15</sup> boron doped diamond (BDD),<sup>49</sup> noble metals, *e.g.* platinum<sup>61</sup> and gold,<sup>62</sup> are much tougher as compared with the conventional carbon fiber.

During the *in vivo* electrochemical detection of targets such as dopamine, by placing CFME near the stimulated dopamine cells, dopamine rapidly diffuses to the electrode, and finally the physical contact of electron transfer can be transformed. This electrode usually consists of about 2.5–7  $\mu\text{m}$  tip diameter, the carbon fiber is sealed in a glass capillary, and the length extending out of the capillary is about 100  $\mu\text{m}$ .<sup>63,64</sup> A peak signal will be generated in the potentiostatic current detection of the electrode. In this signal, the rising part is due to dopamine oxidation after contact with the electrode surface (Fig. 8), and the falling part is due to the decrease of surrounding dopamine concentration due to the influence of absorption and diffusion of the electrode.<sup>65</sup>

Shaneelchandra *et al.*<sup>15</sup> have developed a carbon electrode whose structure is similar to a conical shape. It is deposited by hot acryloyl zinc acetylene and quartz capillary or carbon at the bottom.<sup>66–68</sup> Recent simulation experiments<sup>69</sup> show that these electrodes are composed of tip diameters of 2–5  $\mu\text{m}$ . It is pulled around the capillary tube with an axial length of 4  $\mu\text{m}$ . Compared with CFMEs, the tapered-tip carbon electrode has a fine tip, so *in vivo* experiments help to penetrate the cell membrane more easily during the implantation process, and its glass substrate has stronger mechanical strength. In addition, the open base edge of the tapered-tip carbon electrode is easier for the analyte to approach the electrode base edge than the insulating plane at the junction of the limited fiber capillary on the carbon fiber electrode. Therefore, the tapered-tip electrode has better mass transfer characteristics. In addition, the tapered tip. The size of the carbon electrode is similar to that of the carbon fiber electrode, and it shows a better signal-to-noise ratio when detecting dopamine *in vivo*.<sup>63</sup>

The adsorption of peptides, lipids and amphiphilic high molecular weight proteins in extracellular fluid will cause electrode contamination, which is a common problem in electrochemical biomaterial measurement *in vivo*. The analyte and electrode surface are prevented by the electrochemical pollution, which weakens the transient electrode response, which is the direct reason for the reduction of electrode sensitivity and the distortion of volt ampere signal.<sup>70,71</sup> The problem of electrode biofouling has attracted extensive attention of electrochemical researchers. For example, the introduction of thin films such as Nafion<sup>72</sup> is to solve this problem. This kind of electrochemical materials are negatively charged, which can not only prevent electrode biofouling, but also make cationic polyamine selectively enter the electrode surface at physiological pH value.

Recently, Shanel Chandra *et al.* evaluated the effect of phenyl-acetate film-coated tapered tip carbon electrodes on electrode fouling.<sup>73</sup> The results show that the membrane can reduce the fouling rate of the electrode by about two times compared to the bare cone-tip carbon electrode. Similarly, fsdv is often used to prevent electrochemical pollution when detecting and quantifying dopamine *in vivo*.<sup>74–76</sup> In addition, diamond film fixed electrode has been developed as an anti pollution electrochemical sensor. The electrode is composed of small faceted crystals with a size of 100–200 nm and doped with some boron.<sup>74,77–79</sup> The electrode is inert to amphiphilic substances, and because the microcrystals with good facets of diamond film on the electrode are sealed by hydrogen, the electrode produces a non-polar hydrophobic surface. A large number of researchers have proved that this electrode can minimize pollution in the process of target detection *in vivo*.<sup>78</sup> Hydrogenated graphite carbon has also been proved to be similar to diamond electrode and is not easy to be polluted by amphiphilic macromolecules. This is because graphite oxide carbon is mainly composed of  $\text{sp}^3$  carbon, so it has a similar structure to diamond electrode, so it will be polluted.<sup>80</sup> Some preliminary results of anti scaling *in vitro* using hydrogenated carbon electrode have been reported by Shanel Chandra and colleagues.<sup>66</sup> The electrode was hydrogenated by remote plasma hydrogenation process, and then the hydrogenated electrode was incubated in 0.1% BSA for 3 weeks, so that the hydrogenated carbon electrode was finally formed. The dopamine CV of the bare carbon electrode shows a limiting current of 29%, which is a very serious phenomenon, while the hydrogenated carbon electrode can reduce the limiting current by 5%, so it is an electrode that can promote the electrochemical progress *in vivo*. Interestingly, with the continuous development of electrode hydrogenation technology, Shanel Chandra *et al.*



Fig. 9 SEM image of the BDD microelectrode. The image shows the tip of the needle shaped BDD microelectrode. Figure from Ste'phane Fierro *et al.*<sup>49</sup> Reproduced with permission from *Sci. Rep.*, 2012, 2. Copyright nature Ltd (2012).



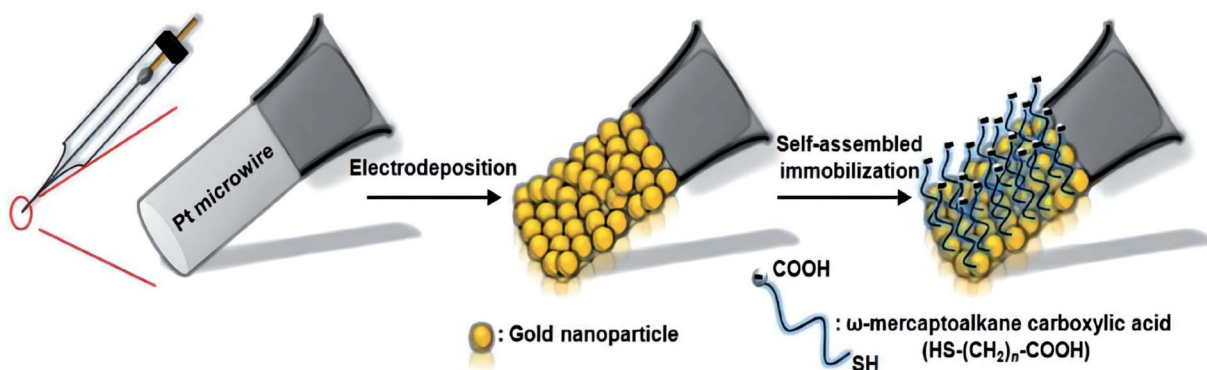


Fig. 10 Schematic illustration of the proposed fabrication process for surface modification of Au-NP/SAMs on the platinum microelectrodes. Figure from Tien-Chun Tsai *et al.*<sup>61</sup> Reproduced with permission from *Analyst*, 2012, 137. Copyright Royal Society of Chemistry (2012).

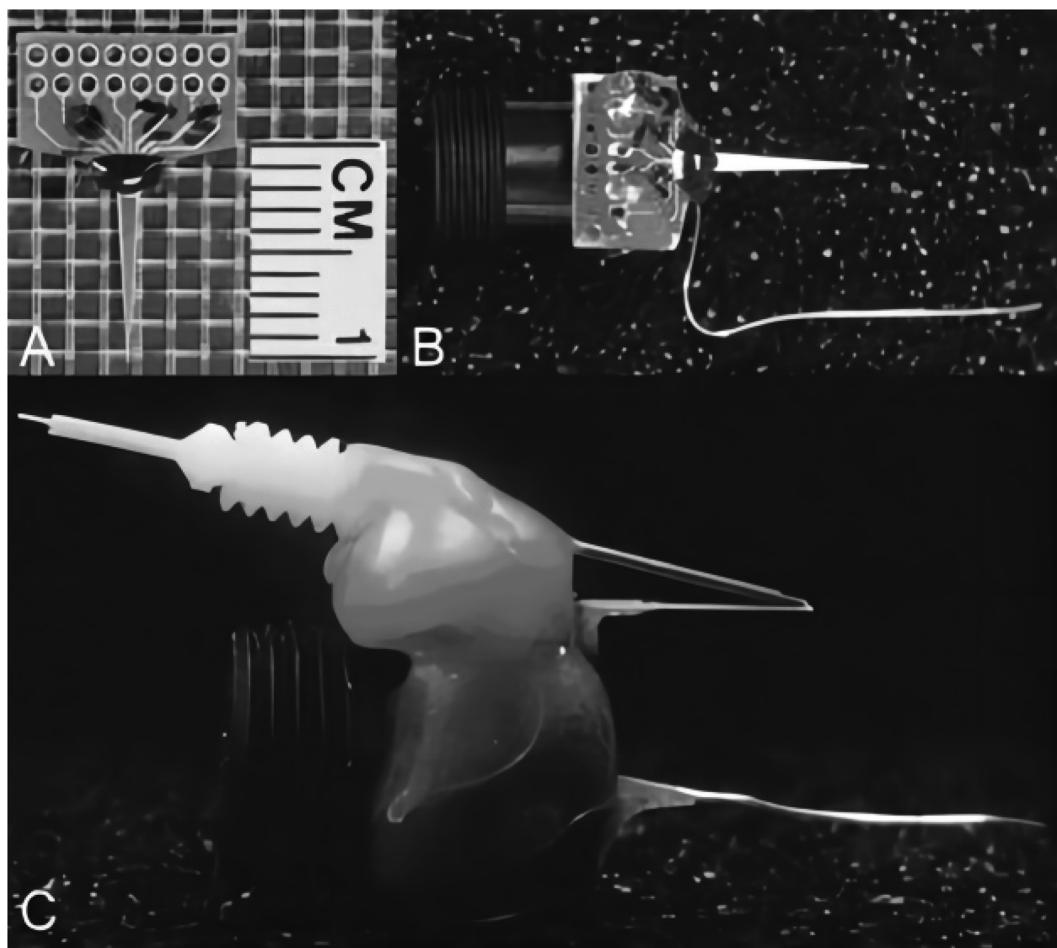


Fig. 11 MEA modification: photographs of the MEA modification process for chronic implantation in the freely moving mouse. (A) Stub MEA with a 1 cm ruler for size comparison. (B) Copper wires are soldered onto the paddle, one for each corresponding platinum recording site. Female, gold sockets are soldered to the other ends of the copper wire, which are inserted into a miniature black connector along with a miniature silver/silver chloride wire. Five-minute epoxy is applied to hold the apparatus together and keep the ceramic tip of the MEA parallel to the miniature black connector for stereotaxic placement. This entire apparatus is now referred to as the pedestal MEA. (C) Side view of (B) with an attached stainless steel guide cannula. Sticky Wax (Kerr Brand, Romulus, MI) was used to hold a guide cannula in place that positions an internal cannula among the four platinum recording sites resting approximately 100  $\mu$ m above the recording surface. Figure from K. N. Hascup *et al.*<sup>91</sup> Reproduced with permission from *J. Pharmacol. Exp. Ther.*, 2008, 324. Copyright Williams & Wilkins Ltd (2008).

Table 3 Properties of the different micro-electrodes electrochemical sensors for *in vivo* measurement

Working electrodes	Enzymes	Experimental model	implantation site	Analytes	Dynamic linear range	detection limit	linear coefficient	Ref.
<b>CFME wire-connected electrochemical <i>in vivo</i> measurements on animals</b>								
CFME/Au/Ni-NTA/E2Zn <sub>2</sub> SOD CFME/Au/Echt	SOD	Rat	Striatum	Cu <sup>2+</sup>	10 nmol L <sup>-1</sup> to 35 μmol L <sup>-1</sup>	3 nmol L <sup>-1</sup>	0.999	10
The MWNT-modified CFME		Male Guinea pigs (350–400 g)	The basal turn of scala tympani VNC	Ascorbate	1 μmol L <sup>-1</sup> to 50 μmol L <sup>-1</sup>	0.999	88	
CFME		The wandering third instar drosophila	PAM region	Dopamine	0.1 to 20 μmol L <sup>-1</sup>	90 nmol L <sup>-1</sup> , 0 nmol L <sup>-1</sup>	0.998 and 0.999	53
Cylindrical carbon-fiber microelectrode CONH <sub>2</sub> -CNT and COOH-CNT-modified electrodes		The Canton-S strain of <i>D. melanogaster</i> Homozygous larvae (3 days)	VNC	Serotonin	0.1 to 20 μmol L <sup>-1</sup>	90 nmol L <sup>-1</sup> , 0 nmol L <sup>-1</sup>	0.998 and 0.999	54
CFME/Au/MPA		Adult male wistar rats (300–350 g)	Hippocampus; striatum; cortex	pH	5.9 to 8.0			55
CFME/Au CFME wire-connected electrochemical <i>in vivo</i> measurements on plants								89
Hb/SWCNTs/CFUME		Aloe	Leaves	H <sub>2</sub> O <sub>2</sub>	4.90–405 μmol L <sup>-1</sup>	4 μmol L <sup>-1</sup>	0.996	14
<b>CFME wireless electrochemical <i>in vivo</i> measurements on animals</b>								
Nafion-nmCFE		Male sprague dawley rats (250–300 g)	Prefrontal cortex	Dopamine 5-HT				58
<b>The glass substrates of conical tip carbon electrodes</b>								
The glass substrates of conical tip carbon, electrode boron doped diamond (BDD) microelectrode		Male sprague dawley rats (303–330 g)	The left striatum	Dopamine	0.2–2.0 μmol L <sup>-1</sup>	721 pmol L <sup>-1</sup>	0.998	15
BDD microelectrode		Nude mice	Subcutaneous	GSH	0–80 mmol L <sup>-1</sup>	0.3 mmol L <sup>-1</sup>	0.998	49
<b>Metallic materials microelectrode</b>								
Au-NP/MPA modified microelectrode			Striatum	Dopamine	0.01–5 μmol L <sup>-1</sup>	7 nmol L <sup>-1</sup>	0.99	61
Poly-TTICA/DGPD/Cyt c/ Au microelectrode		Adult male sprague dawley rats (200–250 g)	The central part of the dorsal striatum	O <sub>2</sub> <sup>•-</sup>	0.2–6.0 nmol L <sup>-1</sup>	30.0 ± 0.9 pmol L <sup>-1</sup>	0.998 and 0.999	62
Snmol/L/CFME		Adult male sprague dawley rats (300–350 g)	Hippocampus	O <sub>2</sub>				109
PTA-PANI-coated CFES		Adult sprague dawley rats (male, 300–350 g)	Nucleus accumbens (NAc)	Dopamine				110



Table 3 (Contd.)

Working electrodes	Enzymes	Experimental model	Implantation site	Analytics	Dynamic linear range	detection limit	linear coefficient	Ref.
Flexibly integrated microelectrode PEDOT/CNT functionalized microelectrodes	GOD	Adult male wistar rats	The skin of cervical dorsal	Glucose	0–20 mmol L <sup>-1</sup>	0.99	111	
Platinum wire working electrodes		Male sprague dawley rats (350–450 g)	Dorsal striatum	Dopamine	2.03 ± 0.09 nmol L <sup>-1</sup>		112	
		Glutamate oxidase (GlutOx), ascorbate oxidase (AsOx)	Male sprague dawley rats(250–350 g)	Subthalamic nucleus (STN)	Glutamate	5 to 150 μmol L <sup>-1</sup>	0.044 μmol L <sup>-1</sup>	0.9979
Cu2S/RGO-CFMEs			The drosophila under good conditions	Dopamine	0.1–20 μmol L <sup>-1</sup>	24 nmol L <sup>-1</sup>	0.993	114
The GOD MPS-/CNT@GHM biosensor electrode	GOD	Male sprague dawley rats (170 g)	Back	Glucose	0 to 24 mmol L <sup>-1</sup>		0.9993	115
Bare or modified KSC paste microelectrodes (denoted as KSCMEds)	GOD	Male pathogen-free wistar rats (200–220 g) and kunning (KM) mice (18–22 g)	Under the skin of the neck	Glucose	0.03–10.0 nmol L <sup>-1</sup>	10 μmol L <sup>-1</sup>	0.999	116

designed a hydrogenated conical carbon electrode probe that can reduce dopamine detection pollution *in vivo* by hydrogenating the conical carbon electrode.<sup>15</sup> This kind of electrode can generate hydrophobic  $sp^3$  carbon surface after hydrogenation, so as to prevent the adsorption of proteins, peptides and amphiphilic substances in extracellular fluid. Therefore, the electrochemical pollution caused by adsorption can be minimized.

### 3.3 Boron doped diamond (BDD) microelectrode

BDD is composed of a particularly hard electrode material<sup>81</sup>, in addition, compared with other traditional electrode materials, it has other outstanding electrode properties such as high resistance to biological and chemical pollution (Fig. 9), low background current, weak adsorption of polar molecules and wide electrochemical potential window.<sup>74,82–85</sup> BDD microelectrode<sup>49</sup> has been used by Ste'phane Fierro *et al.* To detect reduced glutathione (*l*-*c*-glutamyl-*l*-cysteyl-glycine, GSH) *in vivo* and *in vitro*, then it can be used to evaluate the potential application of cancerous tumors. Their study demonstrated the biological characteristics and malignancy of tumors using several *in vivo* measurements of GSH in normal tissues.

It is worth thinking that although BDD has the characteristics of anti biological and chemical pollution, once the BDD electrode is polluted, the current difference between measurements in normal tissue and tumor tissue decreases, resulting in measurement error. Ste'phane Fierro *et al.* Solved this problem by adopting the strategy of cathode treatment (23 V, 20 minutes) in 0.1 M PBS between each measurement. In addition, reliable results can be obtained if the current measurement *in vivo* does not last for more than 5 s.<sup>49</sup> This fully shows that biological pollution is a very serious problem in electrochemical detection *in vivo*.

In all current *in vivo* electrochemical studies, most of them are the detection of brain biological substances.<sup>10,58,63</sup> But in terms of practicality, as with the diagnosis of diabetes, the dynamic detection of subcutaneous glucose is as practical as the acquisition of striatal glucose. Subcutaneous glucose testing focuses on helping us quickly and effectively understand the effects of the body, while the testing of striatal glucose focuses on helping us understand the molecular mechanism of action in the brain. This peripheral tissue GSH measurement method will broaden the field and increase the usefulness of *in vivo* electrochemical research.

### 3.4 Metallic materials microelectrode

Since mechanical strength is the primary consideration in the manufacture of *in vivo* target sensing microelectrodes, Md. Aminur Rahman *et al.* have proposed to make *in vivo* detection microelectrodes with metal materials.<sup>61,62,86</sup> Tien Chun Tsai *et al.*<sup>61</sup> in order to reduce the interference of AA and improve the specificity and sensitivity to DA (Fig. 10), they developed a new microelectrode by modifying platinum microelectrodes with gold nanoparticles (Au NPs) and self-assembled monolayers (SAMs). The robustness, sensitivity and pollution resistance of the sensor can be significantly improved by changing the components and materials of the electrode. To some extent, the selection of appropriate coating is absolutely important to

enhance the electrode characteristics. In this case, the results show that the platinum microelectrode coated with gold nanoparticles and 3-mercaptopropionic acid (MPA) is coated with appropriate coating w-the chain length of mercaptoalkane carboxylic acid can significantly improve the electrode properties, including anti albumin adhesion and fast response time (less than 2 seconds). At the same time, the specificity of Au NP/MPA for AA is about 881 times. During current measurement, its sensitivity is 2.7 times higher than that of traditional Nafion coated electrode.

Different from the inherent properties of chemical contamination resistance of BDD,<sup>49</sup> the change of the structure of the tapered tip carbon electrode after hydrogenation, its electrode surface is susceptible to contamination by protein adhesion.<sup>15</sup> In order to reduce the pollution of negatively charged albumin (isoelectric point, pI 4.7)<sup>87</sup> in the physiological environment, this study used MPA carboxylic acid to solve this problem. At the same time, their study also showed that after using MPA carboxylic acid, Au NP/MPA modified microelectrode soaked in albumin solution for one week did not affect the sensitivity of DA measurement (Fig. 11).

The performance of a microelectrode sensor relatively relies on the fine processing technology. It is crucial to fabricate a tough, good conductivity, fouling resistance microelectrode, and of course, a good coated material is also important (Table 3).

#### 4. Microelectrode arrays (MEA)

The discovery and progress of ceramic based multipoint arrays were described in detail by Gerhardt and colleagues in 2000.<sup>90</sup> This kind of electrode consists of four  $50 \times 50 \mu\text{m}$ . Spacing is  $200 \mu\text{m}$ . Because the ceramic material used in this kind of electrode has stronger mechanical strength than silicon, it is more robust than ordinary microelectrodes. At present, MEA has become an ideal electrode for electrochemical measurement *in vivo*. The wire of the electrode is insulated with polyimide coating, the connecting wire and electrode are made of platinum, and the whole MEA electrode is made by lithography. Remove the ceramic containing the electrode from the wafer of the electrode and make it into a 1 cm long substrate, which can gradually become a  $2\text{--}5 \mu\text{m}$  tip. The selectivity, response time and sensitivity of the electrode are usually expressed by hydrogen peroxide and dopamine voltammetry. Then, the detection of neurotransmitters such as glutamate can be realized by modifying MEA array to manufacture enzyme coated electrode. The team mainly studied the production of glutamate emitters, which is the beginning of the development of non electroactive emitters. In recent years, with the development of electrochemical sensors, the combined determination and rapid measurement technology of glucose, glutamate and acetylcholine can be detected by MEA. In order to eliminate unwanted anions, the team can also carry out *in vivo* electrochemical detection by coating Nafion on four platinum electrodes on the ceramic chip of the electrode.<sup>91</sup>

Glutaraldehyde and BSA are added to each pair of electrodes to crosslink the platinum recording site and glutamate oxidase

(GluOx). The concentration of BSA is 1%, and the electrodes are coated with a mixture of the above three. The preparation of such electrodes is based on the oxidation of glutamate to  $\text{H}_2\text{O}_2$  by GluOx and  $\alpha$ -ketoglutarate, and then  $\text{H}_2\text{O}_2$  can be oxidized by a two electron oxidation process at an electrode potential of 0.7 V *vs.* Ag/AgCl. At present, microelectrode array (MEA) has been widely used for rapid measurement of glutamate. At the same time, MEA can realize continuous and feasible measurement of glutamate in freely moving and awake rats within seven days. In this study, glutamate levels can be significantly reduced by the use of TTX, while elevated glutamate levels can be achieved by local use of DL soviet formula- $\beta$ -hydroxyaspartic acid (THA) was achieved, and these works have been clearly demonstrated by them (Fig. 4). Therefore, because mea electrode can provide fast time resolution and high spatial resolution in glutamate measurement, it is considered to be the most suitable electrode by the team. Resting glutamate levels could not be measured by *in vivo* voltammetry. Through the behavioral development of long-term implantation experiment, it can be seen that *in vivo* electrochemical measurement may be able to measure the resting level of the transmitter. Prefrontal cortex has been reported to be an important brain region related to depression, drug addiction and mental diseases, and it plays an important role in the process of higher cognition (Table 4).

In order to simultaneously monitor acetylcholine and glutamate *in vivo*, gerhart's team expanded the ceramic microarray technology.<sup>92</sup> At the same time, they also monitored the resting level and the dynamic level of stimulus release. In their study, they found that the dynamic and resting levels of each neurotransmitter in any region of the brain were basically similar. For each sub region of the brain, the resting level of acetylcholine was significantly lower than that of glutamate. In the subregion they studied, the level of acetylcholine was significantly higher than that of glutamate induced by KCl, but the release of acetylcholine was slower. At present, the development of biosensor manufacturing and design for glucose level detection in tears has been reported. Tears have become a biological fluid of great concern because of its advantages of noninvasive sampling and detection, and the good correlation between glucose level in tears and blood glucose. Glucose level can be detected by oxidation of glucose by glucose oxidase modified electrode. Recently, scientists have designed an electrochemical biosensor that can efficiently collect 5 mL sample of tears. Its preparation principle is to insert a complete sensor into the capillaries.<sup>93</sup> The sensor uses rabbit tears to detect blood glucose levels. It is worth noting that the glucose oxidase modified flexible platinum electrode of the sensor is loaded on the eye lens made of biocompatible polymer.<sup>94</sup> At the same time, compared with other sensors, a reverse/reference electrode is designed on the polymer substrate. Through the above technology, the real-time detection of glucose can be realized, and there will be little or no stimulation to animals. Through the correlation analysis between tear and blood glucose level in rabbits, Ming Xing Chua and her colleagues found that the blood glucose level changed with the change of tear glucose level, but there was a 10 minute delay between them (Table 5).



Table 4 Properties of different MEA for *in vivo* measurement

Working electrodes	Biosensor material	Enzymes	Experimental model	Monitoring site	Analytics	Dynamic linear range	detection limit	Linear coefficient	Ref.
A flexible Pt working electrode	Biocompatible 2-methacryloyloxyethyl phosphorylcholine (MPC) polymer and polydimethyl siloxane (PDMS)	GOD	Rabbit	Eye	Glucose	0.03–5.0 mmol L <sup>-1</sup>	0.999	94	
Immobilizing GOD on a 0.25 mm o.d. platinum/iridium (Pt/Ir) wire								93	
Four platinum recording sites	Ceramic based conformal MEAs	GluOx AChE ChOx	Male fischer 344 rats (28–32 g)	mPFC	Glutamate ACh				
Enzyme layers coated onto the surface of platinum (Pt) recording sites	Ceramic based conformal MEAs	GluOx	Male C57BL/6 mice (28–32 g)	Prefrontal, cortex striatum	l-Glutamate	0.1–2 mmol L <sup>-1</sup>	0.9 ± 0.2 μmol L <sup>-1</sup>	92	
Au/Cr or Pt/Cr	A polyimide-film substrate		Male sprague-dawley rats (300–400 g)	The spinal cord dorsal horn				91	
The Pt nanoparticles modified microelectrode	Silicon-substrate	GOx2mPD	A male sprague-Dawley rat (270 g)	Striatum	l-Glutamate			8	
MEA sensor recording site working electrode	Platinum nanoparticles and reduced graphene oxide nanocomposites (Pt/rGO)		Male sprague-dawley rats (250 g)	Caudate putamen (CPU)	Glucose	0–23 mmol L <sup>-1</sup>	0.998	96	
Consisting of the electrochemical recording site	Silicon-based microelectrode array (MEA)	Gluox	Male sprague-dawley rats (250–300 g)	Hippocampus cornu Ammoni/	Dopamine	50 nmol L <sup>-1</sup> –16.3 μmol L <sup>-1</sup>	0.999	117	
RgDAAO coated MEA	d-Amino acid oxidase from the yeast rhodotorula gracilis (RgDAAO)		Male long Evans rat (15 weeks)	Lon 1 (CA1)	Glutamate	0–50 μmol L <sup>-1</sup>	0.5 μmol L <sup>-1</sup>	0.9986	
				Prefrontal cortex	d-Serine		0.17 ± 0.01 μmol L <sup>-1</sup>	118	
A four-shank implantable microelectrode array (MEA)	SWCNTs/PEDOT:PSS-modified MEAs		Sprague dawley rats	Striatum	Dopamine	10 nmol L <sup>-1</sup> –72 μmol L <sup>-1</sup>	10 nmol L <sup>-1</sup>	120	
Ceramic-based multisite Pt microelectrode arrays (MEAs)			Male wistar rat(300 g)	Parietal cortex	O <sub>2</sub>	0–25 μmol L <sup>-1</sup>	0.33 ± 0.20 μmol L <sup>-1</sup>	121	

Table 5 Comparison of advantages and disadvantages of different methods for electrochemical *in vivo* detection

Methods	Advantages	Disadvantages	Ref.
MD-electrochemical <i>in vivo</i> detection system	<p>This method is relatively mature</p> <p>This method can long time monitoring</p> <p>Multiple components can be simultaneously detected after combined with microfluidic chip</p>	<p>The microdialysis probe is expensive</p> <p>The dialysis membrane is easy to be blocked and difficult to be reused</p> <p>Because of its long tubings, this method is not the very real-time detection, and the experimental animals require anesthetized or fixed</p>	22, 26–34, 45, 47 and 48
Micro-electrodes electrochemical <i>in vivo</i> detection system	<p>This method can make a <i>in situ</i> real time detection <i>in vivo</i></p> <p>Combined with the wireless sensing device, this system can monitor the chemicals in freely behaving animals</p> <p>Microelectrode array can simultaneously detect multiple components</p>	<p>The manufacturing process of microelectrodes is very complicated</p> <p>The sensor is easily contaminated</p> <p>To get accurate results, the <i>in vivo</i> detection time cannot be long</p>	8, 10, 15, 49, 57, 58, 61, 62 and 88

An integrated flexible implantable probe was developed by hung Cao *et al.*<sup>8</sup> on polyimide film substrate and used for the detection of neurotransmitters. Because the probe is very flexible, it can effectively reduce the trauma to the tissue during implantation, so the probe can realize long-term detection *in vivo*. At the same time, Pt/Cr or Au/Cr working electrode and micro Ag/AgCl reference electrode are integrated in the probe, so there is no need for a separate reference electrode in the measurement process. At present, several electrodes for implantation in different positions of the central nervous system have been used. The enzyme based electrochemical L-glutamic acid sensor of L-glutamic acid oxidase is a prototype device with proof of principle. The selectivity can be significantly improved by depositing L-glutamic acid oxidase on the working electrode and then electropolymerizing *m*-phenylenediamine. Their performance as working electrodes can be evaluated by comparing Au and Pt films by CV. At the same time, the selectivity and detection limit can be improved by using self reference technology. Regardless of the presence of interfering molecules, the assembled and assembled sensors can show good selectivity and sensitivity under different concentrations of L-glutamate. By inserting a sensor probe into the dorsal horn of the spinal cord for *in vivo* animal experiments, the ability to detect changes in electrochemical signals in response to graded peripheral somatosensory stimulation is due to the termination of nociceptive primary afferent fibers.<sup>95</sup>

Currently, the technology of MEA is not yet mature, especially in terms of multi-component detection. It is the same with micro-electrode electrochemical sensors that the fine processing technologies are their main challenge.

## 5. Conclusions and outlook

Microdialysis has been applied in many fields. It is a mature sampling technology for monitoring biological compounds *in vivo*. MD-electrochemical system is currently the most accurate

and the longest time *in vivo* detection technique. Because of its maturity and stability, man will be able to use it to screen drugs, research chemicals such as neurotransmitters changes after external stimuli. Moreover, the development of manufacturing technology has greatly promoted the progress of innovative microchip technology for real-world monitoring applications.

With the continuous development of electrochemical analysis, the function of electrochemical detection *in vivo* is also increasing. The catabolism of neurotransmitters after animal administration has been shifted from microdialysis to microchip electrophoresis and microelectrodes.<sup>133</sup> The research mainly uses microdialysis technology. The disadvantage of this method is that it needs to be used in combination with classical liquid phase methods such as high performance liquid phase, and cannot realize real-time quantitative detection of drug catabolism. Microchip electrophoresis and microelectrode solve this problem very well. At the same time, at present, *in vivo* electrochemistry can only indirectly reflect the influence of drug metabolism by detecting neurotransmitter metabolism, and there is no electrochemical research directly targeting drug metabolism *in vivo*. The disadvantages of traditional pharmacokinetics also make the detection of drug metabolism *in vivo* more real-time and accurate.

In addition, with the emergence of nanomaterials, nanotechnology has greatly promoted the development of *in vivo* electrochemistry.<sup>134</sup> At present, electrochemical biosensors for *in vivo* detection of ROS have also been developed. Such sensors have real-time detection, low cost,<sup>135</sup> and rapid response., high sensitivity and selectivity. However, there are no *in vivo* electrochemical studies on food-borne pathogens or food-borne toxins, and only a few *in vitro* studies.<sup>136</sup> Therefore, it is very urgent for us to develop biosensors for food-borne pathogens or toxins, and we also believe that this is also the future of electrochemistry. One of the main directions of chemical development.



With the development of microfluidic chip technology, MD-electrochemical sensors will be able to simultaneously detect more chemicals *in vivo*, and through the development of new semipermeable membrane, man will create the new dialysis membrane which is low cost and could resist the macromolecules adhesion in the extracellular fluid and could be reused easily in the future. The microelectrode electrochemical *in vivo* detection system is a real-time *in situ* detection method in the living body, combined with wireless sensing devices, can dynamically monitor the chemical substances in plants and freely moving animals. In particular, Qiongqiong Ren and colleagues<sup>45</sup> realized electrochemical monitoring in plants by modifying carbon fiber ultramicroelectrodes (CFUME) and single-walled carbon nanotubes (SWCNT). Although the use of modified CFUME for the measurement of chemical substances in plants has the advantages of low interference and easy data processing, the effective real-time monitoring time in plants is still not as good as that in animals. In addition, there are many plants such as albumin and other electrochemical biofouling. For chemical pollutants, it is urgent to develop some electrochemical sensors that are resistant to pollution and can monitor plants for a long time.

Through the development of new coatings or the transformation of the electrode surface morphology, finding new micro-electrode materials, people have minimized the foulings at the micro-electrodes, and maximized the detected time. But it is still an arduous task to greatly extend the monitoring time and get accurate results simultaneously. It is still an urgent need to develop a stable, reliable and powerful electrochemical platform that can meet all the requirements of biological samples and recognition elements. Nowadays, many researchers are making great efforts to resist sensor fouling from biological media.<sup>97</sup> Therefore, we have reason to believe that a surface chemistry platform which combines high binding capacity and retention of specificity and activity of bio-recognition elements (e.g. antibodies or DNA) with high resistance to non-specific binding will be built up in the near future.

At present, implantable and self-powered electrochemical sensors have also been developed. Such sensors can obtain energy from living organisms, such as the chemical energy of heartbeat, respiration, and glucose redox reaction.<sup>130</sup> This shows that the online MD-electrochemical biosensor system and microelectrode-electrochemical *in vivo* detection system will not be limited to basic research such as brain substances. The analysis of this kind of *in vivo* brain chemicals has also made major breakthroughs in the application research of human subcutaneous blood glucose monitoring. Therefore, we look forward to more *in vivo* analysis and an increase in the actual application rate in the future.

With the development of the electrochemical *in vivo* measurement, the ability to acquire direct physiological information will bridge the gap between observed living creatures behaviors and the chemical signaling pathways that underlie those behaviors.

With the continuous development of electrochemical biosensors, it can be seen that microdialysis, microchip and microelectrode equipment are constantly optimized and the

research on membrane manufacturing alternative materials is deepening. At present, due to the emerging use of self-powered electrochemical sensors, the integrated procedures and manufacturing of implantable/wearable MD/microelectrode systems for animal monitoring have also been developed.<sup>129,130</sup> I believe that electrochemical sensors will continue to broaden and deepen the field of *in vivo* research. Moreover, electrochemical sensors will develop towards faster and more sensitive measurement, more selective detection of possible molecular targets, and smaller and more compact electrode arrays. At the same time, the focus of electrochemical detection in the field of *in vivo* research will be on more control over the system to be measured. Finally, it is expected that electrochemical sensors can achieve great breakthroughs in translational medicine and biological substance analysis, thereby further improving the level of human medical treatment.

## Conflicts of interest

There are no conflicts to declare.

## Acknowledgements

Zhangjiagang Health Commission Youth Project (guidance) (ZKY2019036), Research Fund of Zhangjiagang first people's Hospital (ZKY201852), Natural Science Foundation of Jiangxi Province (20212BAB206012).

## References

- 1 D. Su, K. Bi, C. Zhou, Y. Song, B. Wei, L. Geng, W. Liu and X. Chen, *Chromatographia*, 2010, **71**, 603.
- 2 D. Su, Y. Song, L. Geng, B. Wei, P. Xie, Y. Qi, C. Ma, S. Yang, K. Bi and X. Chen, *Chromatographia*, 2011, **73**, 1189.
- 3 Y. Song, D. Su, T. Lu, C. Mao, D. Ji, Y. Liu, B. Wei and R. Fan, *J. Sep. Sci.*, 2014, **37**, 352.
- 4 Y. Liu, Y. Song, Q. Xu, D. Su, Y. Feng, X. Li, I. A. Khan, L. Zhang, L. Chen and S. Yang, *J. Chromatogr. B: Anal. Technol. Biomed. Life Sci.*, 2013, **141**, 942–943.
- 5 B. Xu, S. Gao, B. Wu, T. Yin and M. Hu, *J. Pharm. Biomed. Anal.*, 2014, **88**, 180.
- 6 E. E. Chambers, M. J. Woodcock, J. P. Wheaton, T. M. Pekol and D. M. Diehl, *J. Pharm. Biomed. Anal.*, 2014, **88**, 660.
- 7 Y. Lin, K. Spiller, R. Aras and W. Jian, *J. Pharm. Biomed. Anal.*, 2022, **213**, 114697.
- 8 H. Cao, A.-L. Li, C. M. Nguyen, Y.-B. Peng and J.-C. Chiao, *IEEE Sens. J.*, 2012, **12**, 1618.
- 9 L. Wang, Q. Zhang, S. Chen, F. Xu, S. Chen, J. Jia, H. Tan, H. Hou and Y. Song, *Anal. Chem.*, 2014, **86**, 1414.
- 10 X. Chai, X. Zhou, A. Zhu, L. Zhang, Y. Qin, G. Shi and Y. Tian, *Angew. Chem.*, 2013, **52**, 8129.
- 11 A. Ravalli, G. Marrazza, L. Rivas, A. De La Escosura-Muniz and A. Merkoci, in *Sensors and Microsystems*, Springer, 2014, p. 175.
- 12 Y. Wan, Y. Su, X. Zhu, S. Yang, J. Lu, J. Gao, C. Fan and Q. Huang, *Biosens. Bioelectron.*, 2014, **55**, 231.



13 W. Si, W. Lei, Z. Han, Y. Zhang, Q. Hao and M. Xia, *Sens. Actuators, B*, 2014, **193**, 823.

14 Q. Q. Ren, X. J. Yuan, X. R. Huang, W. Wen, Y. D. Zhao and W. Chen, *Biosens. Bioelectron.*, 2013, **50**, 318.

15 S. Chandra, A. D. Miller, A. Bendavid, P. J. Martin and D. K. Wong, *Anal. Chem.*, 2014, **86**, 2443.

16 L. Z. Bito and H. Davson, *Exp. Neurol.*, 1966, **14**, 264.

17 L. Bito, H. Davson, E. Levin, M. Murray and N. Snider, *J. Neurochem.*, 1966, **13**, 1057.

18 P. Hashemi, R. Bhatia, H. Nakamura, J. P. Dreier, R. Graf, A. J. Strong and M. G. Boutelle, *J. Cereb. Blood Flow Metab.*, 2009, **29**, 166.

19 D. Feuerstein, A. Manning, P. Hashemi, R. Bhatia, M. Fabricius, C. Tolias, C. Pahl, M. Ervine, A. J. Strong and M. G. Boutelle, *J. Cereb. Blood Flow Metab.*, 2010, **30**, 1343.

20 U. Ungerstedt, *J. Intern. Med.*, 1991, **230**, 365.

21 M. Zhang, K. Liu, K. Gong, L. Su, Y. Chen and L. Mao, *Anal. Chem.*, 2005, **77**, 6234.

22 X. Lu, H. Cheng, P. Huang, L. Yang, P. Yu and L. Mao, *Anal. Chem.*, 2013, **85**, 4007.

23 B. V. d. Araújo, J. V. Laureano, L. D. Grünspan, T. D. Costa and L. Tasso, *J. Chromatogr. B: Anal. Technol. Biomed. Life Sci.*, 2013, **919**, 62.

24 Z. Liu, M. Liu, Y. Qi, Z. Zhu, Y. Chai, C. Yuan and Y. Lin, *J. Sep. Sci.*, 2013, **36**, 1659.

25 J. Westerhout, D.-J. van den Berg, R. Hartman, M. Danhof and E. de Lange, *Eur. J. Pharm. Sci.*, 2014, **57**, 11.

26 W. Ma, Q. Jiang, P. Yu, L. Yang and L. Mao, *Anal. Chem.*, 2013, **85**, 7550.

27 K. Liu, P. Yu, Y. Lin, Y. Wang, T. Ohsaka and L. Mao, *Anal. Chem.*, 2013, **85**, 9947.

28 X. Zhuang, D. Wang, Y. Lin, L. Yang, P. Yu, W. Jiang and L. Mao, *Anal. Chem.*, 2012, **84**, 1900.

29 H. Gu, Y. Yu, X. Liu, B. Ni, T. Zhou and G. Shi, *Biosens. Bioelectron.*, 2012, **32**, 118.

30 Y. Yu, Q. Sun, T. Zhou, M. Zhu, L. Jin and G. Shi, *Bioelectrochemistry*, 2011, **81**, 53.

31 Y. Yu, X. Liu, D. Jiang, Q. Sun, T. Zhou, M. Zhu, L. Jin and G. Shi, *Biosens. Bioelectron.*, 2011, **26**, 3227.

32 G. S. Laura, M. Borland, H. Yang and A. C. Michael, *J. Neurosci. Methods*, 2005, **146**, 149.

33 Y. Xin, Z. Zhang, P. Yu, F. Ma and L. Mao, *Sci. China: Chem.*, 2013, **56**, 256–261.

34 L. Li, Y. Zhang, J. Hao, *et al.*, *Analyst*, 2016, 2199.

35 X. Xu, S. Zhang, H. Chen and J. Kong, *Talanta*, 2009, **80**, 8.

36 A. Manz, N. Gruber and H. á. Widmer, *Sens. Actuators, B*, 1990, **1**, 244.

37 A. T. Woolley, K. Lao, A. N. Glazer and R. A. Mathies, *Anal. Chem.*, 1998, **70**, 684.

38 R. Tantra and A. Manz, *Anal. Chem.*, 2000, **72**, 2875.

39 R. Ferrigno, J. N. Lee, X. Jiang and G. M. Whitesides, *Anal. Chem.*, 2004, **76**, 2273.

40 B. Graß, A. Neyer, M. Jöhnck, D. Siepe, F. Eisenbeiß, G. Weber and R. Hergenröder, *Sens. Actuators, B*, 2001, **72**, 249.

41 J. E. Prest, S. J. Baldock, N. Bektaş, P. R. Fielden and B. J. Treves Brown, *J. Chromatogr. A*, 1999, **836**, 59.

42 J. E. Prest, S. J. Baldock, P. R. Fielden and B. J. T. Brown, *The Analyst*, 2001, **126**, 433.

43 C. Ma, N. M. Contento, L. R. Gibson and P. W. Bohn, *Anal. Chem.*, 2013, **85**, 9882.

44 C. Ma, N. M. Contento, L. R. Gibson and P. W. Bohn, *ACS Nano*, 2013, **7**, 5483.

45 J.-H. Park, Y. S. Song, J.-G. Ha, Y.-K. Kim, S.-K. Lee and S. J. Bai, *Sens. Actuators, B*, 2013, **188**, 1300.

46 Y. Lin, X. Lu, X. Gao, H. Cheng, T. Ohsaka and L. Mao, *Electroanalysis*, 2013, **25**, 1010.

47 X. Gao, P. Yu, Y. Wang, T. Ohsaka, J. Ye and L. Mao, *Anal. Chem.*, 2013, **85**, 7599.

48 B.-U. Moon, M. G. de Vries, C. A. Cordeiro, B. H. Westerink and E. Verpoorte, *Anal. Chem.*, 2013, **85**, 10949.

49 S. Fierro, M. Yoshikawa, O. Nagano, K. Yoshimi, H. Saya and Y. Einaga, *Sci. Rep.*, 2012, **2**, 901.

50 M. Benoit-Marand, M. Jaber and F. Gonon, *Eur. J. Neurosci.*, 2000, **12**, 2985.

51 J. J. Burmeister, F. Pomerleau, P. Huettl, C. R. Gash, C. E. Werner, J. P. Bruno and G. A. Gerhardt, *Biosens. Bioelectron.*, 2008, **23**, 1382.

52 J. E. Quintero, B. K. Day, Z. Zhang, R. Grondin, M. L. Stephens, P. Huettl, F. Pomerleau, D. M. Gash and G. A. Gerhardt, *Exp. Neurol.*, 2007, **208**, 238.

53 X. Borue, S. Cooper, J. Hirsh, B. Condron and B. J. Venton, *J. Neurosci. Methods*, 2009, **179**, 300.

54 M. A. Makos, Y.-C. Kim, K.-A. Han, M. L. Heien and A. G. Ewing, *Anal. Chem.*, 2009, **81**, 1848.

55 C. B. Jacobs, T. L. Vickrey and B. J. Venton, *The Analyst*, 2011, **136**, 3557.

56 J. Liu, P. Yu, Y. Lin, N. Zhou, T. Li, F. Ma and L. Mao, *Anal. Chem.*, 2012, **84**, 5433.

57 Q.-Q. Ren, X.-J. Yuan, X.-R. Huang, W. Wen, Y.-D. Zhao and W. Chen, *Biosens. Bioelectron.*, 2013, **50**, 318.

58 F. Crespi, *Biosens. Bioelectron.*, 2010, **25**, 2425.

59 V. Annovazzi-Lodi and S. Donati, *IEEE Trans. Biomed. Eng.*, 1991, **38**, 212.

60 M. F. Roitman, G. D. Stuber, P. E. Phillips, R. M. Wightman and R. M. Carelli, *J. Neurosci.*, 2004, **24**, 1265.

61 T. C. Tsai, C. X. Guo, H. Z. Han, Y. T. Li, Y. Z. Huang, C. M. Li and J. J. Chen, *Analyst*, 2012, **137**, 2813.

62 M. A. Rahman, A. Kothalam, E. S. Choe, M. S. Won and Y. B. Shim, *Anal. Chem.*, 2012, **84**, 6654.

63 D. Kim, S. Koseoglu, B. M. Manning, A. F. Meyer and C. L. Haynes, *Anal. Chem.*, 2011, **83**, 7242.

64 P. R. Miller, S. D. Gittard, T. L. Edwards, D. M. Lopez, X. Xiao, D. R. Wheeler, N. A. Monteiro-Riviere, S. M. Brozik, R. Polksy and R. J. Narayan, *Biomicrofluidics*, 2011, **5**, 013415.

65 D. J. Michael and R. M. Wightman, *J. Pharm. Biomed. Anal.*, 1999, **19**, 33.

66 S. Alwarappan, K. S. A. Butcher and D. K. Wong, *Sens. Actuators, B*, 2007, **128**, 299.

67 M. McNally and D. K. Wong, *Anal. Chem.*, 2001, **73**, 4793.



68 D. Wong, C. Blaha and M. McNally, *Chem. Aust.*, 2003, **70**, 12.

69 D. Britz, S. Chandra, J. Strutwolf and D. K. Wong, *Electrochim. Acta*, 2010, **55**, 1272.

70 J. Park, V. Quaiserová-Mocko, B. A. Patel, M. Novotný, A. Liu, X. Bian, J. J. Galligan and G. M. Swain, *Analyst*, 2008, **133**, 17.

71 N. J. Finnerty, S. L. O'Riordan, E. Palsson and J. P. Lowry, *J. Neurosci. Methods*, 2012, **209**, 13.

72 G. A. Gerhardt, A. F. Oke, G. Nagy, B. Moghaddam and R. N. Adams, *Brain Res.*, 1984, **290**, 390.

73 S. Chandra, A. D. Miller and D. K. Wong, *Electrochim. Acta*, 2013, **101**, 225.

74 K. Yoshimi, Y. Naya, N. Mitani, T. Kato, M. Inoue, S. Natori, T. Takahashi, A. Weitemier, N. Nishikawa and T. McHugh, *Neurosci. Res.*, 2011, **71**, 49.

75 P. A. Garris, R. Enzman, J. Poehlman, A. Alexander, P. E. Langley, S. G. Sandberg, P. G. Greco, R. M. Wightman, G. V. Rebec and J. Neurosci, *Methods*, 2004, **140**, 103.

76 S. Hafizi, Z. L. Kruk and J. A. Stamford, *J. Neurosci. Methods*, 1990, **33**, 41.

77 S. Wang, V. M. Swope, J. E. Butler, T. Feygelson and G. M. Swain, *Diamond Relat. Mater.*, 2009, **18**, 669.

78 F. Shang, L. Zhou, K. A. Mahmoud, S. Hrapovic, Y. Liu, H. A. Moynihan, J. D. Glennon and J. H. Luong, *Anal. Chem.*, 2009, **81**, 4089.

79 Y. S. Singh, L. E. Sawarynski, H. M. Michael, R. E. Ferrell, M. A. Murphey-Corb, G. M. Swain, B. A. Patel and A. M. Andrews, *ACS Chem. Neurosci.*, 2009, **1**, 49.

80 J. Datta, N. R. Ray, P. Sen, H. S. Biswas and E. A. Vogler, *Mater. Lett.*, 2012, **71**, 131.

81 C. Prado, G.-U. Flechsig, P. Gründler, J. S. Foord, F. Marken and R. G. Compton, *Analyst*, 2002, **127**, 329.

82 T. Yano, D. Tryk, K. Hashimoto and A. Fujishima, *J. Electrochem. Soc.*, 1998, **145**, 1870.

83 R. Trouillon and D. O'Hare, *Electrochim. Acta*, 2010, **55**, 6586.

84 R. Trouillon, D. O'Hare and Y. Einaga, *Phys. Chem. Chem. Phys.*, 2011, **13**, 5422.

85 A. Suzuki, T. A. Ivandini, K. Yoshimi, A. Fujishima, G. Oyama, T. Nakazato, N. Hattori, S. Kitazawa and Y. Einaga, *Anal. Chem.*, 2007, **79**, 8608.

86 M. A. Rahman, A. Kothalam, E. S. Choe, M.-S. Won and Y.-B. Shim, *Anal. Chem.*, 2012, **84**, 6654.

87 I. Vlasova and A. Saletsky, *J. Appl. Spectrosc.*, 2009, **76**, 536.

88 J. Liu, P. Yu, Y. Lin, N. Zhou, T. Li, F. Ma and L. Mao, *Anal. Chem.*, 2012, **84**, 5433.

89 F. Zhao, L. Zhang, A. Zhu, *et al.*, *Chem. Commun.*, 2016, **52**, 3717.

90 K. N. Hascup, E. R. Hascup, F. Pomerleau, P. Huettl and G. A. Gerhardt, *J. Pharmacol. Exp. Ther.*, 2008, **324**, 725.

91 C. E. Mattinson, J. J. Burmeister, J. E. Quintero, F. Pomerleau, P. Huettl and G. A. Gerhardt, *J. Neurosci. Methods*, 2011, **202**, 199.

92 Q. Yan, B. Peng, G. Su, B. E. Cohan, T. C. Major and M. E. Meyerhoff, *Anal. Chem.*, 2011, **83**, 8341.

93 M. X. Chu, K. Miyajima, D. Takahashi, T. Arakawa, K. Sano, S.-i. Sawada, H. Kudo, Y. Iwasaki, K. Akiyoshi and M. Mochizuki, *Talanta*, 2011, **83**, 960.

94 E. R. Kandel, J. H. Schwartz and T. M. Jessell, *Principles of neural science*, McGraw-Hill, New York, vol. 4, 2000.

95 W. Wei, Y. Song, X. Fan, *et al.*, *Nanotechnology*, 2016, **27**, 114001.

96 H. Vaisocherová, V. Ševčík, P. Adam, B. Špačková, K. Hegnerová, A. de los Santos Pereira, C. Rodriguez-Emmenegger, T. Riedel, M. Houska and E. Brynda, *Biosens. Bioelectron.*, 2014, **51**, 150.

97 R. A. Saylor and S. M. Lunte, PDMS/glass hybrid device with a reusable carbon electrode for on-line monitoring of catecholamines using microdialysis sampling coupled to microchip electrophoresis with electrochemical detection, *Electrophoresis*, 2018, **39**(3), 462–469.

98 S. M. Gunawardhana and S. M. Lunte, Continuous monitoring of adenosine and its metabolites using microdialysis coupled to microchip electrophoresis with amperometric detection, *Anal. Methods*, 2018, **10**(30), 3737–3744.

99 Y. Jiang, W. Ma, W. Ji, H. Wei and L. Mao, Aptamer superstructure-based electrochemical biosensor for sensitive detection of ATP in rat brain with *in vivo* microdialysis, *Analyst*, 2019, **144**(5), 1711–1717.

100 Y. Jiang, X. Xiao, C. Li, Y. Luo, S. Chen, G. Shi, K. Han and H. Gu, Facile Ratiometric Electrochemical Sensor for *in vivo*/Online Repetitive Measurements of Cerebral Ascorbic Acid in Brain Microdialysate, *Anal. Chem.*, 2020, **92**(5), 3981–3989.

101 B. Li, L. Li, K. Wang, C. Wang, L. Zhang, K. Liu and Y. Lin, Ultrasensitive and facile electrochemical detection of hydrogen sulfide in rat brain microdialysate based on competitive binding reaction, *Anal. Bioanal. Chem.*, 2017, **409**(4), 1101–1107.

102 T. N. H. Nguyen, J. K. Nolan, H. Park, S. Lam, M. Fattah, J. C. Page, H. E. Joe, M. B. G. Jun, H. Lee, S. J. Kim, R. Shi and H. Lee, Facile fabrication of flexible glutamate biosensor using direct writing of platinum nanoparticle-based nanocomposite ink, *Biosens. Bioelectron.*, 2019, **131**, 257–266.

103 K. Zhang, X. He, Y. Liu, P. Yu, J. Fei and L. Mao, Highly Selective Cerebral ATP Assay Based on Micrometer Scale Ion Current Rectification at Polyimidazolium-Modified Micropipettes, *Anal. Chem.*, 2017, **89**(12), 6794–6799.

104 J. Liu, Y. Zhang, M. Jiang, L. Tian, S. Sun, N. Zhao, F. Zhao and Y. Li, Electrochemical microfluidic chip based on molecular imprinting technique applied for therapeutic drug monitoring, *Biosens. Bioelectron.*, 2017, **91**, 714–720.

105 S. M. Gunawardhana, G. A. Bulgakova, A. M. Barybin, S. R. Thomas and S. M. Lunte, Progress toward the development of a microchip electrophoresis separation-based sensor with electrochemical detection for on-line *in vivo* monitoring of catecholamines, *Analyst*, 2020, **145**(5), 1768–1776.

106 W. Tedjo, J. E. Nejad, R. Feeny, L. Yang, C. S. Henry, S. Tobet and T. Chen, Electrochemical biosensor system



using a CMOS microelectrode array provides high spatially and temporally resolved images, *Biosens. Bioelectron.*, 2018, **114**, 78–88.

107 Z. Pu, J. Tu, R. Han, X. Zhang, J. Wu, C. Fang, H. Wu, X. Zhang, H. Yu and D. Li, A flexible enzyme-electrode sensor with cylindrical working electrode modified with a 3D nanostructure for implantable continuous glucose monitoring, *Lab Chip*, 2018, **18**(23), 3570–3577.

108 Z. Pu, J. Tu, R. Han, X. Zhang, J. Wu, C. Fang, H. Wu, X. Zhang, H. Yu and D. Li, A flexible enzyme-electrode sensor with cylindrical working electrode modified with a 3D nanostructure for implantable continuous glucose monitoring, *Lab Chip*, 2018, **18**(23), 3570–3577.

109 L. Zhou, H. Hou, H. Wei, L. Yao, L. Sun, P. Yu, B. Su and L. Mao, *in vivo* Monitoring of Oxygen in Rat Brain by Carbon Fiber Microelectrode Modified with Antifouling Nanoporous Membrane, *Anal. Chem.*, 2019, **91**(5), 3645–3651.

110 T. Feng, W. Ji, Q. Tang, H. Wei, S. Zhang, J. Mao, Y. Zhang, L. Mao and M. Zhang, Low-Fouling Nanoporous Conductive Polymer-Coated Microelectrode for *in vivo* Monitoring of Dopamine in the Rat Brain, *Anal. Chem.*, 2019, **91**(16), 10786–10791.

111 Y. Fang, S. Wang, Y. Liu, Z. Xu, K. Zhang and Y. Guo, development of Cu nanoflowers modified the flexible needle-type microelectrode and its application in continuous monitoring glucose *in vivo*, *Biosens. Bioelectron.*, 2018, **110**, 44–51.

112 I. M. Taylor, N. A. Patel, N. C. Freedman, E. Castagnola and X. T. Cui, Direct *in vivo*Electrochemical Detection of Resting Dopamine Using Poly(3,4-ethylenedioxothiophene)/Carbon Nanotube Functionalized Microelectrodes, *Anal. Chem.*, 2019, **91**(20), 12917–12927.

113 M. Ganesana, E. Trikantzopoulos, Y. Maniar, S. T. Lee and B. J. Venton, development of a novel micro biosensor for *in vivo* monitoring of glutamate release in the brain, *Biosens. Bioelectron.*, 2019, **130**, 103–109.

114 B. Zhang, C. Li, H. Zhang, Y. Chen, H. Jiang, L. Chen, F. Ur Rehman and X. Wang, *in vivo* Dopamine Biosensor Based on Copper(I) Sulfide Functionalized Reduced Graphene Oxide Decorated Microelectrodes, *J. Biomed. Nanotechnol.*, 2018, **14**(7), 1277–1286.

115 H. Huang, T. Li, M. Jiang, C. Wei, S. Ma, D. Chen, W. Tong and X. Huang, Construction of flexible enzymatic electrode based on gradient hollow fiber membrane and multi-wall carbon tubes meshes, *Biosens. Bioelectron.*, 2020, **152**, 112001.

116 Y. Song, D. Su, Y. Shen, H. Liu and L. Wang, Design and preparation of open circuit potential biosensor for *in vitro* and *in vivo* glucose monitoring, *Anal. Bioanal. Chem.*, 2017, **409**(1), 161–168.

117 G. Xiao, Y. Song, Y. Zhang, Y. Xing, H. Zhao, J. Xie, S. Xu, F. Gao, M. Wang, G. Xing and X. Cai, Microelectrode Arrays Modified with Nanocomposites for Monitoring Dopamine and Spike Firings under Deep Brain Stimulation in Rat Models of Parkinson's Disease, *ACS Sens.*, 2019, **4**(8), 1992–2000.

118 Z. Li, Y. Song, G. Xiao, F. Gao, S. Xu, M. Wang, Y. Zhang, F. Guo, J. Liu, Y. Xia and X. Cai, Bio-electrochemical microelectrode arrays for glutamate and electrophysiology detection in hippocampus of temporal lobe epileptic rats, *Anal. Biochem.*, 2018, **550**, 123–131.

119 D. Campos-Beltrán, Å. Konradsson-Geuken, J. E. Quintero and L. Marshall, Amperometric Self-Referencing Ceramic Based Microelectrode Arrays for D-Serine Detection, *Biosensors*, 2018, **8**(1), 20.

120 E. He, S. Xu, Y. Dai, Y. Wang, G. Xiao, J. Xie, S. Xu, P. Fan, F. Mo, M. Wang, Y. Song, H. Yin, Y. Li, Y. Wang and X. Cai, SWCNTs/PEDOT:PSS-Modified Microelectrode Arrays for Dual-Mode Detection of Electrophysiological Signals and Dopamine Concentration in the Striatum under Isoflurane Anesthesia, *ACS Sens.*, 2021, **6**(9), 3377–3386.

121 A. Ledo, C. F. Lourenço, J. Laranjinha, C. M. Brett, G. A. Gerhardt and R. M. Barbosa, Ceramic-Based Multisite Platinum Microelectrode Arrays: Morphological Characteristics and Electrochemical Performance for Extracellular Oxygen Measurements in Brain Tissue, *Anal. Chem.*, 2017, **89**(3), 1674–1683.

122 H. T. Nguyen, M. Massino, C. Keita and J. B. Salmon, Microfluidic dialysis using photo-patterned hydrogel membranes in PDMS chips, *Lab Chip*, 2020, **20**(13), 2383–2393.

123 J. Liu, W. Lu, L. Zhang, J. Yang, Z. P. Yao, Y. He and Y. Li, Integrated hand-held electrochemical sensor for multicomponent detection in urine, *Biosens. Bioelectron.*, 2021, **193**, 113534.

124 J. Wang, J. Wen and H. Yan, Recent Applications of Carbon Nanomaterials for microRNA Electrochemical Sensing, *Chem.-Asian J.*, 2021, **16**(2), 114–128.

125 C. Wang, X. Bi, M. Wang, X. Zhao and Y. Lin, Dual-Channel Online Optical Detection Platform Integrated with a Visible Light Absorption Approach for Continuous and Simultaneous *in vivo* Monitoring of Ascorbic Acid and Copper(II) Ions in a Living Rat Brain, *Anal. Chem.*, 2019, **91**(24), 16010–16016.

126 K. Liu, P. Yu, Y. Lin, Y. Wang, T. Ohsaka and L. Mao, Online electrochemical monitoring of dynamic change of hippocampal ascorbate: toward a platform for *in vivo* evaluation of antioxidant neuroprotective efficiency against cerebral ischemia injury, *Anal. Chem.*, 2013, **85**(20), 9947–9954.

127 A. C. Valenta, C. I. D'Amico, C. E. Dugan, J. P. Grinias and R. T. Kennedy, A microfluidic chip for on-line derivatization and application to *in vivo* neurochemical monitoring, *Analyst*, 2021, **146**(3), 825–834.

128 P. Wonnenberg, W. Cho, F. Liu, T. Asrat and A. G. Zestos, Polymer Modified Carbon Fiber Microelectrodes for Precision Neurotransmitter Metabolite Measurements, *J. Electrochem. Soc.*, 2020, **167**(16), 167507.

129 S. Santiago-Malagón, D. Río-Colín, H. Azizkhani, M. Aller-Pellitero, G. Guirado and F. J. Del Campo, A self-powered skin-patch electrochromic biosensor, *Biosens. Bioelectron.*, 2021, **175**, 112879.



130 D. Jiang, B. Shi, H. Ouyang, Y. Fan, Z. L. Wang and Z. Li, Emerging Implantable Energy Harvesters and Self-Powered Implantable Medical Electronics, *ACS Nano*, 2020, **14**(6), 6436–6448.

131 S. P. Butcher, I. S. Fairbrother, J. S. Kelly and G. W. Arbuthnott, Effects of selective monoamine oxidase inhibitors on the in vivo release and metabolism of dopamine in the rat striatum, *J. Neurochem.*, 1990, **55**(3), 981–988.

132 M. P. Brazell, C. A. Marsden, A. P. Nisbet and C. Routledge, The 5-HT1 receptor agonist RU-24969 decreases 5-hydroxytryptamine (5-HT) release and metabolism in the rat frontal cortex in vitro and in vivo, *Br. J. Pharmacol.*, 1985, **86**(1), 209–216.

133 K. M. Schilly, S. M. Gunawardhana, M. B. Wijesinghe and S. M. Lunte, Biological applications of microchip electrophoresis with amperometric detection: in vivo monitoring and cell analysis, *Anal. Bioanal. Chem.*, 2020, **412**(24), 6101–6119.

134 S. Zhao, G. Zang, Y. Zhang, H. Liu, N. Wang, S. Cai, C. Durkan, G. Xie and G. Wang, Recent advances of electrochemical sensors for detecting and monitoring ROS/RNS, *Biosens. Bioelectron.*, 2021, **179**, 113052.

135 A. N. Vaneev, P. V. Gorelkin, A. S. Garanina, H. V. Lopatukhina, S. S. Vodopyanov, A. V. Alova, O. O. Ryabaya, R. A. Akasov, Y. Zhang, P. Novak, S. V. Salikhov, M. A. Abakumov, Y. Takahashi, C. R. W. Edwards, N. L. Klyachko, A. G. Majouga, Y. E. Korchev and A. S. Erofeev, In Vitro and In Vivo Electrochemical Measurement of Reactive Oxygen Species After Treatment with Anticancer Drugs, *Anal. Chem.*, 2020, **92**(12), 8010–8014.

136 M. Amiri, A. Bezaatpour, H. Jafari, R. Boukherroub and S. Szunerits, Electrochemical Methodologies for the Detection of Pathogens, *ACS Sens.*, 2018, **3**(6), 1069–1086.

137 Y. Zhang, J. Xiao, Y. Sun, L. Wang, X. Dong, J. Ren, W. He and F. Xiao, Flexible nanohybrid microelectrode based on carbon fiber wrapped by gold nanoparticles decorated nitrogen doped carbon nanotube arrays: In situ electrochemical detection in live cancer cells, *Biosens. Bioelectron.*, 2018, **100**, 453–461.

